

Bio-climatic factors drive spectral vegetation changes in Greenland

Tiago Silva^{1,2}, Brandon Samuel Whitley³, Elisabeth Machteld Biersma³, Jakob Abermann^{1,2},
Katrine Raundrup⁴, Natasha de Vere³, Toke Thomas Høye^{5,6}, Verena Haring⁷, and Wolfgang Schöner^{1,2}

¹Geography and Regional Science Institute, University of Graz, Graz, Austria

²Austrian Polar Research Institute, Vienna, Austria

³Natural History Museum of Denmark, University of Copenhagen, Copenhagen, Denmark

⁴Department of Environment and Minerals, Greenland Institute of Natural Resources, Nuuk, Greenland

⁵Department of Ecoscience, University of Aarhus, Aarhus, Denmark

⁶Arctic Research Centre, University of Aarhus, Aarhus, Denmark

⁷Institute of Biology, University of Graz, Graz, Austria

Correspondence: Tiago Silva (tiago.ferreira-da-silva@uni-graz.at)

Abstract.

The terrestrial Greenland ecosystem (ice-free area) has undergone significant changes over the past decades, affecting biodiversity. Changes in ~~air-temperature~~ near-surface air temperature and precipitation have modified the duration and conditions of snowpack during the cold season, altering ecosystem interactions and functioning. In this study, we statistically aggregated the
5 Copernicus Arctic regional reanalysis (CARRA) and ~~remotely-sensed-spectral-vegetation-data~~ remotely sensed spectral data on green vegetation, spanning from 1991 to ~~2023-by-using-2023~~ 2023. We use principal component analysis (PCA) ~~in-order-to-I-~~ to examine key sub-surface and above-surface bio-climatic factors influencing ecological and phenological processes preceding and during the thermal growing season in tundra ecosystems; ~~H. interpret-~~ Subsequently, we interpreted spatio-temporal interactions among bio-climatic factors on vegetation ~~across-Greenland~~; ~~III. investigate-and-investigated~~ bio-climatic changes
10 dependent on ~~location-and-elevation-in-Greenland~~; ~~IV. identify~~ latitude and topographical features in Greenland. Ultimately, we described regions of ongoing changes in green vegetation distribution.

~~Consistent-with-other-studies-~~ Our results show that green vegetation has responded highly to the prevailing weather patterns of the past decades, particularly along West Greenland. The PCA effectively clustered bio-climatic indicators that co-vary with summer spectral vegetation, demonstrating the potential of CARRA for biogeographic studies. The duration of the thermal
15 growing season (GrowDays) emerged as the pivotal factor across all ecoregions (with increases up to 10 days per decade), interacting with other bio-climatic indicators to promote summer vegetation growth. ~~Regions-with-significant-snow-height-decrease~~ The lengthening of GrowDays is explained by reduced winter precipitation associated with warming (up to 1.5°C per decade). Significant decreases in snow height occur along with ~~an-earlier-snowmelt-period~~ earlier snowmelt (up to 20 days per decade), ~~which-triggers-the~~ leading to an earlier onset of GrowDay~~earlier~~. ~~In-most-regions,-we-find-that-shallower-snowpacks-tend-to~~ melt slower. ~~We-hypothesise-that-slow-snowmelt-rates-foster-microbial-activity,-enriching-the-soil-with-nutrients.-The-combined-effect-of-soil-nutrients-and-the-resulting-warming-in-spring-(up-to-1.5°C-per-decade)-,-promotes-early-plant-development.-These~~ We find that regions with shallower snowpacks, experiencing slower snowmelt rates during the ablation period, are linked with a higher soil water content in spring; this relation not only coincides with the greenest regions in West and Southwest

Greenland, but also with regions where green vegetation has recently emerged. Such processes occur prior to GrowDays and were combined with summer weather conditions that favoured warmer and clear-skies that resulted in significant summer greening. The relatively warmer and drier summer conditions experienced in the northern and interior of the studied regions evidenced surface thawing and drying. Despite these summer bio-climatic ~~changes, in the cold and summer season, have led to interlinks green vegetation expanded~~ northward and upward ~~vegetation expansion. The distribution of~~. Green vegetation has expanded in Northeast Greenland by 22.5% ~~increase~~ with respect to ~~2008–2023~~ 1991–2007 period, leading to new vegetated areas. We report little to no change in the length and onset of the GrowDays along the coast in Northeast Greenland, in contrast with more pronounced changes inland and at higher elevations, hence showing an elevation-dependent response (increases up to 5 days per decade per km elevation). Our ~~study determines a set of statistical outcomes and interpretations derived from reanalysis and remote sensing data that include uncertainties, are corroborated by in situ studies conducted in the tundra region. The~~ bio-climatic indicators ~~relevant for understanding vegetation. These insights provide a basis to validate and the associated insights serve not only as a foundation for validating~~ bio-climatic indicators from climate models to assess future ~~vegetation changes across Greenland under a changing~~ changes in vegetation, but they also advocate for the inclusion of permafrost dynamics schemes. This integration will enhance the quantification of atmosphere-vegetation-permafrost-carbon feedback loops across terrestrial Greenland amid the evolving climate.

1 Introduction

The changing climate in the past decades has profound and rapid effects on Arctic ecosystems, with regional ~~Greenland warming~~ warming in Greenland at nearly three times the global average (Rantanen et al., 2022). This rapid warming is causing significant changes in the region's climate patterns and ecosystems. Jansen et al. (2020) highlight that the current era of abrupt climate change in the Arctic is unprecedented in the context of the past several thousand years, leading to complex and varied responses in Arctic vegetation. Myers-Smith et al. (2020) reveal the intricacies of ~~the~~ "Arctic greening", where increased temperatures and earlier snowmelt drive changes in plant growth and species distribution. These changes affect ecological interactions, such as shifts in plant community composition ~~, and~~ alterations in soil nutrient cycling, leading to feedback mechanisms involving snow cover and surface albedo. Similarly, Huang et al. (2017) discuss the rate of change in vegetation productivity across northern high latitudes, reiterating that the response to climate change is influenced by multiple factors, including soil moisture availability, temperature variations, and the timing and extent of snowmelt.

Over the last three decades, community plant height has increased across the Arctic (~~Metealfe et al., 2018~~) (Bjorkman et al., 2018). This has largely been caused by plant community changes, in particular due to an increase in abundance and productivity of deciduous shrub species – causing “shrubification” of the tundra (~~Sturm et al., 2001~~) (e.g., Mekonnen et al. 2021; Sturm et al. 2001). A large-scale study on the interconnection between temperature, moisture, and various key plant functional traits at 117 Arctic locations over 30 years of warming revealed a strong relationship between temperature and particular plant traits; however, soil moisture was a strong factor determining the strength and direction of these relationships (~~Metealfe et al. 2018~~) (Bjorkman et al. 2018). Changes in plant communities ~~and the expansion of deciduous shrubs with warmer~~

~~summers are likely are also~~ reliant on the availability of soil moisture (e.g., Ackerman et al. 2017; Gamm et al. 2018; Power et al. 2024), ~~exhibiting a rapid rise in deciduous shrubs in wet regions, but a decline in dry tundra zones.~~ Studies on dynamic tundra vegetation future scenarios have suggested that the expansion of deciduous shrubs is favored by warmer summers, whereas graminoids are more likely to increase in wetter conditions (van der Kolk et al., 2016).

Due to high latitude and continentality, summer soil moisture availability is particularly important in certain areas of Greenland ~~that are already drier than other parts~~. In these drier areas, higher temperatures and less precipitation during the summer can potentially cause desiccation and salt accumulation at the soil surface, with a negative effect on plant growth (Zwolicki et al., 2020). Therefore, it is expected that an increase in temperature will unlikely lead to a striking increase in plant growth, mainly due to the lack of precipitation. For instance, a study on growth responses of two widespread and dominant deciduous shrub species (*Salix glauca* L. and *Betula nana* L.) in western Greenland ~~, using dendrochronology, stable isotope analysis, and leaf gas exchange measurements~~ revealed that both species have declined in growth since the 1990s, likely due to increasing water limitation (Gamm et al., 2018). However, increasing herbivory also plays a role, such as increased moth outbreaks (Post and Pedersen, 2008), ~~a growing muskoxen population~~ growing muskoxen populations in West (Eikelenboom et al., 2021) and East Greenland (Schmidt et al., 2015) and increases in geese populations in East Greenland (Boertmann et al., 2015). Such studies are however based on small-scale ~~analysis and in analyses and~~ contrast with observations of increasing shrub growth in other parts of the Arctic (Metcalf et al., 2018). Also, certain inland parts of Greenland are warmer and drier than most other areas of the Arctic, and will therefore respond differently to climate change. ~~Therefore,~~ making their spatial representativeness ~~is unclear~~. The critical influence of soil water availability on future changes in tundra plant communities in Greenland should not be underestimated, and may also serve as an indicator for other drier Arctic regions, which may experience similar changes in temperature and precipitation. Additionally, while certain plant communities ~~such as the evergreen dwarf shrubs~~ are generally better adapted to drier conditions, and have been observed to have increased with recent warming in the colder and drier High Arctic (~~Weijers et al., 2017~~) (e.g., Heijmans et al. 2022; Opała-Owczarek et al. 2018; Weijers et al. 2017), it is likely that ~~these certain~~ species also become decreasingly temperature- and increasingly soil moisture-dependent during summer (Weijers, 2022).

Temperature, precipitation, as well as soil water availability during the growing season are a few of the climatic indicators contributing to vegetation changes (Migala et al., 2014). However, other climatic indicators, such as snowfall, ~~snow cover melt~~ snowmelt rate and timing and frost also play an important role even before the onset of the growing season (Cooper, 2014). The projected ~~warmer temperatures for increase in temperatures during~~ the cold season will likely have a ~~very different effect~~ than different impact on vegetation that warmer temperatures during the growing season (Weijers, 2022). Increased snow depth during the cold season usually ~~means increased causes increased plant~~ growth in the following summer, as more snow provides insulation, less frost damage and ~~an~~, depending on the snowpack characteristics, increase in water availability ~~in the spring~~ (e.g., Lamichhane 2021; Migala et al. 2014; Wang et al. 2024). ~~Also, increased insulation has been shown to lead to an increased microbial breakdown of leaf litter and therefore an enhanced nutrient supply in~~ A relevant characteristic of the snowpack is that deep snow requires more energy to equalise the cold content and the liquid water holding capacity to subsequently initiate and sustain melt than shallow snowpacks (Colbeck 1976; Musselman et al. 2017). As a result, deep snow often subsists for longer

periods, potentially delaying the start of the growing season, which can hinder plant growth (Schmidt et al., 2015). On the other hand, the insulation provided by deep snow has also been demonstrated to promote increased microbial decomposition, enhancing the nutrient supply for the following growing season (e.g., Cooper 2014; Pedron et al. 2023); Xu et al. 2021). The higher amount of energy input needed to melt deep snow means that it melts later but also faster, which can cause nutrient loss through increased runoff. Concurrently, meltwater from relatively shallow snow percolates the soil more efficiently during the ablation period, in contrast with fast snowmelt that quickly saturates the soil surface and runs off (Stephenson and Freeze, 1974). These slow snowmelt rates allow water to remain in the soil for extended periods, which is critical for activating soil microbial communities. These microbes then produce nutrients that are vital for vegetation growth (Glanville et al., 2012). However, if snow is limited and precipitation is falling as rain rather than snow, the resulting ice conditions can have damaging effects on the vegetation (increased branch mortality and vegetation damage, Weijers 2022) and in soil nutrient cycling. Additionally, in exceptional years like 2018, the High Arctic experienced unusually large amounts of snow coverage, resulting in extraordinarily delayed snowmelt. This made it very difficult for plants to grow and for animals to access resources (Schmidt et al., 2019). Such conditions will strongly influence the growth of plants, and have impacts throughout the food chain, such as for the Svalbard reindeer (Le Moullec et al., 2020) and the caribou in West Greenland (Eikelenboom et al., 2021). Overall, the amount of snow and the coupling with temperature are highly important for plant growth, and plant community composition in the Arctic, and a Greenland-focused study assessing bio-climatic changes has not yet been made.

Grimes et al. (2024) has recently shown that the doubling of vegetation across ice-free Greenland is linked with warming. However, the warming observed in Greenland over recent decades has been associated with more frequent and intense weather patterns that promote widespread clear-sky conditions and the advection of relatively warm air masses from southern latitudes along West Greenland (Barrett et al., 2020). Weather patterns can be related to indices by analysing specific atmospheric variables over time and space. For instance, the North Atlantic Oscillation is driven by surface pressure configurations in the North Atlantic (Hurrell et al., 2003), and the Greenland Blocking Index measures geopotential height in the mid-troposphere over Greenland (Hanna et al., 2016). Both indices are commonly utilized in climate studies to deduce influences on various components of the climate system in Greenland and vicinity (e.g., Björk et al. 2018; Olafsson and Rousta 2021). Therefore, how warming impacts other interlinked bio-climatic indicators through weather patterns requires further investigation.

In order to properly assess changes in bio-climatic indicators in Greenland, it is important to consider that soil water sources in the region are mainly from precipitation, snowmelt and permafrost ground thaw. The combination of hard local geology with scouring by the ice sheet has shaped the landscape, and thin soils result in less prevalent thermokarst and low water retention (Anderson 2020). This means that Therefore, meltwater flows rather freely according to the surface gradient, eventually gathering in low-lying areas to form lakes or drains towards the sea. Therefore, tundra vegetation develops in regions adjacent to such water bodies, eventually colonizing recently drained regions (e.g., Chen et al. 2023). Due to climate warming, not only surface, but also subsurface runoff has increased in the Arctic (Rawlins and Karmalkar 2024). The increased runoff in combination with the climate-induced terrestrial greening has led to a decline in nutrients export via rivers to the sea, which decreased phytoplankton biomass in the coastal ecosystems (Sogaard et al., 2023). Given the heterogeneity in soil properties

and water availability sources, sub-surface bio-climatic indicators, such as volumetric soil water and, potentially, sub-surface runoff, should be considered.

In this study, we analyse 32 years (1991–2023) of remotely-sensed Normalized Difference Vegetation Index (NDVI) data to gain a deeper understanding of the spatio-temporal patterns of spectral vegetation changes across ice-free regions of Greenland, extending beyond the representativeness of point-scale studies. ~~Furthermore, we~~ We examine the combined effects of bio-climatic indicators ranging from sub-surface factors (such as soil water availability) to above-surface factors (such as the thermal growing season, heat stress, and frost) with summer spectral greenness. We also extend our study of bio-climatic changes beyond the summer by ~~including~~ examining indicators from the preceding winter and spring ~~, and~~ and assessing their combined impact with summer spectral greenness. Additionally, we explore historical trends of bio-climatic indicators individually ~~, investigating and investigate~~ their latitudinal and ~~altitudinal-topographical~~ sensitivity. Finally, we identify regions with changes in spectral greenness and in greenness distribution.

2 Data

2.1 Copernicus Arctic regional reanalysis

The Copernicus Arctic regional reanalysis (CARRA) system predominantly relies on the non-hydrostatic numerical weather prediction model HARMONIE-AROME (Bengtsson et al., 2017), laterally forced by ERA5. CARRA, with a spatial resolution of 2.5 km, assimilates the same ~~observation~~ observational datasets as ERA5 (Hersbach et al., 2020), supplemented by additional station data from the national meteorological services involved within the CARRA domain. This study employed the CARRA-West domain, which encompasses ~~ice-free~~ Greenland. For the ice-free Greenland domain, the additional station data that CARRA assimilates is sourced from the Danish Meteorological Institute and Asiaq-Greenland Survey networks. However, snow depth observations are not provided and not assimilated by CARRA. According to the CARRA Full System documentation (Schyberg et al., 2020), ice cover extent remains constant throughout the entire reanalysis period (1991–2023). The Leaf Area Index (LAI) climatology in CARRA is updated based on the multi-year mean values from the Moderate Resolution Imaging Spectroradiometer (MODIS) MCD15A2H C6 (Yang et al. 2006; Yuan et al. 2011), and these have been used to update the ECOCLIMAP cover types for Greenland. ECOCLIMAP-I (Masson et al., 2003) is ~~a~~ the global database utilized to initialize the Surface Externalisée (SURFEX, Masson et al. 2013), the soil–vegetation–atmosphere transfer ~~schemes~~ scheme within CARRA. SURFEX is a multi-layer surface model that computes specific schemes dependent on the surface type (e.g., vegetation, soil, snow), allowing soil water phase changes and enabling runoff over frozen and unfrozen soil. This helps to better represent areas with permafrost and ice surfaces in Greenland as they are not well described in the present version of HARMONIE-AROME. Soil properties in CARRA are derived from the Harmonized World Soil Database (Nachtergaele et al., 2010). The CryoClim project has generated a satellite-derived product of snow extent, which provides access to data collected on a daily basis from 1982 to 2015. CryoClim is a worldwide, optical snow product that utilizes the historical Advanced Very High-Resolution Radiometer - Global Area Coverage (AVHRR GAC) data (Stengel et al. 2020). In the context of CARRA, the CryoClim data is ultimately ~~chosen~~ used due to its comprehensive coverage for the entire period up

to 2015. The data providers assure that the data for the period post-2015 have been produced and arranged in collaboration with the CryoClim developers at the Norwegian Meteorological Institute. Despite the fact that neither snow depth nor snow extent is assimilated, van der Schot et al. (2024) demonstrate in a recent study that the agreement is strong between the snow water equivalent modelled by CARRA and a snow model utilizing in situ observations in both the West and East coastal regions of Greenland. They report that CARRA is capable of successfully representing snow-related indicators, with correlation coefficients exceed 0.8 and mean absolute percentage errors less than 30%.

The derived precipitation from CARRA was taken from its underlying model forecast system and is not an assimilated product. Hence, to minimize the impact of the spin up, we followed the CARRA Full System documentation (Schyberg et al., 2020), which suggests combining 12 h accumulated precipitation by the difference of precipitation at lead time 18 and 6 h from forecasts initiated at 00 UTC and 12 UTC. This procedure was used for determining liquid precipitation (time integral of rain flux) and total solid precipitation (time integral of total solid precipitation flux).

2.2 NOAA Climate Data Record for Normalized Difference Vegetation Index

Phenology studies in remote sensing utilize data collected by satellite sensors, which determine the spectrum of light absorbed and reflected by majorly green vegetation. Specific pigments present in plant leaves exhibit a pronounced absorption of visible light wavelengths, particularly those in the red spectrum. Conversely, the leaves exhibit a strong reflection of near-infrared (NIR) light wavelengths. While numerous vegetation indices exist, one of the most prevalent is the Normalized Difference Vegetation Index (NDVI), which uses red and near-infrared bands. NDVI serves as a measure of spectral vegetation health and spans from -1 to 1. Biologically, NDVI values close to +1 suggest a high density of greenness and robust vegetation health, while values near zero indicate barren land or surfaces with little to no vegetation, such as rocks or sand. Negative NDVI values are typically associated with water, clouds, or snow, likely signifying areas with no vegetation presence.

The National Oceanic and Atmospheric Administration (NOAA) Climate Data Record (CDR) using the AVHRR (Vermote et al. 2018) NDVI, Version 5 (hereafter AVHRR NDVI) and NOAA CDR using the Visible Infrared Imager Radiometer Suite (VIIRS, Vermote et al. 2022) NDVI, Version 1 (hereafter VIIRS NDVI) are jointly used in this study from 1991 to 2023 on a daily basis with grid resolution of 0.05 ~~degrees~~ ~~grid resolution~~ ~~degrees~~ (approx. 5.5 km in latitude and around 2.5 and 0.5 km between 60 and 85 degrees North, respectively). AVHRR NDVI is available until the end of 2013, and ~~thereafter-is then is thereafter~~ continued by its successor VIIRS NDVI. The surface reflectance and the associated AVHRR and VIIRS NDVI take into consideration atmospheric corrections (e.g., total column of atmospheric water vapour, ozone, and aerosol optical thickness). According to AVHRR and VIIRS technical reports, the NIR channel is centred at different wavelengths (830 nm vs. 865 nm). As there is no overlapping period available in the NOAA CDR, potential mismatches between AVHRR and VIIRS NDVI cannot be discarded. However, AVHRR NDVI uses the MODIS Land-Sea mask and its cloud mask is spectrally adjusted using 10 years of MODIS data, with 90% match accuracy over land (Franch et al. 2017). As VIIRS will eventually replace MODIS for land science, MODIS is also used to calibrate VIIRS NDVI estimates (Skakun et al. 2018).

~~As both gridded products in this study have different spatial resolutions, spectral greenness from NOAA NDVI is spatially interpolated to the CARRA grid with resolution of 2.5 km. In addition to NDVI, both products provide quality control flags.~~

While the AVHRR NDVI flags the entire domain for latitudes above 60 degrees as polar latitudes, the VIIRS NDVI implements more stringent quality control measures, effectively flagging clouds and snow cover at polar latitudes.

195 2.3 Climatic oscillation indices

A variety of analytic approaches, such as principal component analysis (PCA) or *k*-means clustering, are often utilized to characterize the North Atlantic Oscillation (NAO), with input data sourced either from reanalysis or station records. Here, the NAO derived from sea-level pressure applying PCA is used. In this study, the NAO index calculated applying the leading principal component derived from sea-level pressure anomalies within the Atlantic domain (20°N–80°N, 90°W–40°E) is
200 provided by National Center for Atmospheric Research/University Corporation for Atmospheric Research (NCAR/UCAR) (Hurrell et al., 2003). This product is posited to yield a more comprehensive representation of NAO spatial patterns compared to indices based on specific terrestrial stations. Notwithstanding, it is noteworthy to acknowledge the dynamic nature of PCA-based NAO indices, being subject to ongoing refinement with the integration of new data.

The Greenland Blocking Index (GBI) is derived from 500 hPa geopotential height over the region (60°N–80°N, 80°W–20°W),
205 retrieved from NOAA Physical Sciences Laboratory/Earth System Research Laboratories (PSL/ESRL) (Hanna et al., 2016). Both the NAO and GBI indices originate from the NOAA National Centers for Environmental Prediction (NCEP/NCAR) reanalysis dataset (Kalnay et al. 1996). Consequently, these climatic oscillation indices have undergone seasonal standardization against the baseline period of 1950–2000.

3 Methods

210 3.1 Spectral greenness

Arctic regions are characterized by sparse vegetation, that typically exhibit markedly low NDVI values, often as low as 0.15 (e.g., Gandhi et al. 2015; Liu et al. 2024), with dense shrubs above 0.5 (e.g., Walker et al. 2005), and signal saturation at around 0.7 (e.g., Myers-Smith et al. 2020; Liu et al. 2024; Walker et al. 2005). Based on the daily datasets provided by AVHRR NDVI and VIIRS NDVI, monthly (averaged) NDVI ($\text{monthly NDVI} = \frac{\sum_{n=1}^n \text{NDVI}_i}{n}$, where *n* is the total number of observations in a
215 month) is calculated pixel-wise for days with NDVI ≥ 0.15. Estimates).

As estimates integrated through time are less likely to be influenced by temporal sampling artefacts at high latitudes than metrics based on maximum NDVI (e.g., Myers-Smith et al. 2020). Pixels with monthly NDVI equal or higher than, we started by calculating monthly integrated NDVI. Also, since our focus is on green vegetation, only daily NDVI pixel values higher or equal to 0.15 are also used to determine the interannual extent of vegetation.

220 While AVHRR NDVI only raises a polar flag above 60 degrees of latitude, VIIRS NDVI applies a more strict quality control, effectively flagging not only clouds but also snow at polar latitudes. Consequently, *n* is higher for AVHRR NDVI than for VIIRS NDVI, impacting monthly NDVI for AVHRR NDVI. As pixels with snow cover, clouds and shadow are not flagged in AVHRR are considered. Then, we divide the monthly integrated NDVI by the total number of monthly observations (*n*, see Figure S1

for the interannual variability of n) to obtain the monthly NDVI. However, before 2014 and as described in Subsection 2.2, the AVHRR algorithm was less strict in its data quality control compared to VIIRS from 2014 onward, resulting in higher n before 2014 that lowers monthly NDVI. To address temporal heterogeneities, we adjusted n from the AVHRR period with the number of monthly observations acquired during the VIIRS period. From 2014 to 2023, we identified the minimum, maximum and average number of observations for each month. Hence, using these three quantities, we generated a consistent variability range from 1991 to 2013 to recalculate monthly NDVI, ~~that certainly influenced surface reflectance, we used the monthly minimum, mean and maximum of n from VIIRS for each year between 2014 and 2023 to estimate monthly uncertainty in spectral greenness between 1991 and 2013. In this way, we assume similar occurrence of pixels with~~ to 2023. This procedure assumes that the environmental conditions (i.e. snow-cover, clouds and shadow ~~throughout the study period. Figure S1 presents the monthly spatial extent (number of observations multiplied by area) recorded by~~) between 1991 to 2013 are similar to those between 2014 and 2023. The maps for the average number of monthly observations and the associated standard deviation for AVHRR and VIIRS ~~from 1991~~ period before and after the adjustment regarding n are shown in Figures S2-S5, respectively.

Pixels with monthly NDVI equal to or greater than 0.15, representative of the area covered by green vegetation, are used to estimate the extent of green vegetation. We applied this same definition to compare how often certain pixels were classified as areas with green vegetation from 2008 to 2023 ~~across all ecoregions to ensure comparable interannual spatial coverage versus~~ the earlier period from 1991 to 2007. We refer to this comparison as changes in greenness distribution. Finally, we calculated a seasonally averaged NDVI, hereafter referred to as spectral greenness and interchangeably as green vegetation.

As both gridded products in this study have different spatial resolutions, spectral greenness from NOAA NDVI is spatially interpolated to the CARRA grid with resolution of 2.5 km.

3.2 Bio-climatic factors

The set of chosen bio-climatic indicators were inspired by previous work from Aalto et al. (2023) and Rantanen et al. (2023), who proposed and investigated bioclimatic indices in Finland and across the Arctic. Our study emphasizes Greenland, considering adapted thresholds and additional climatic factors.

Table 1. Brief description of the bio-climatic indicators derived in the study.

Bio-climatic Indicator	Description
T _{2m}	seasonally averaged air-temperature <u>air temperature</u> at the height of 2 m above the surface
SWE _{MAX}	mass of liquid water from melting the snow per unit area
SWE _{MAX} DOY	day of the year for SWE _{MAX}
SnowDays	snow-covered days when SWE is higher than 10 mm w.e.
GrowDays	days with daily T _{2m} higher than 1 °C that does not belong to SnowDays
DegreeDays	sum of daily T _{2m} during GrowDays
Onset	first day of GrowDays
End	last day of GrowDays
MeltRate	fraction of SWE_{MAX} by the number of <u>mean melt rate for ablation</u> days between SWE _{MAX} DOY and Onset of GrowDays
Greenness	seasonally averaged monthly NDVI, as described in Section 3.1
Snow	seasonally accumulated mass per unit area of snow and ice particles falling on the surface
RainRatio	fraction of liquid precipitation <u>out</u> of the total precipitation
RainOnSnow	RainRatio higher than 50% in SnowDays
Rain	<u>seasonally accumulated mass per unit area of rain falling on the surface, when RainRatio>50%</u>
VPd	vapour pressure deficit is the difference between the amount of water vapour in the air and the amount of water vapour the air can <u>could</u> hold when it is saturated
VSI	seasonally averaged water equivalent of volumetric soil ice content
VSW	seasonally averaged volumetric liquid water in the soil
FrostDays	SWE lower than 10 mm w.e. in spring with negative daily T _{2m}
DroughtDays	days with precipitation lower than 1 mm w.e. lasting for more than 10 consecutive days
HeatDays	days exceeding the seasonal T _{2m} climatology for the period 1991-2023 by 2 SD
Longitude	distance east or west of the Greenwich meridian
Latitude	distance north of the equator
Elevation	vertical elevation above sea level
Surface slope	<u>the inclination of the surface</u>
Surface aspect	<u>the slope direction</u>

Surface slope is transformed into sine aspect (west-east orientation) and cosine aspect (north-south orientation), given its circular orientation. Positive values in sine (cosine) aspect indicate how much the slope is facing east (north), whereas negative values indicates how much the slope is facing west (south).

From CARRA daily-averaged snow water equivalent (SWE), we derived the maximum SWE (SWE_{MAX}), the day of the year SWE_{MAX} occurs (SWE_{MAX} DOY) and snow-covered days (SnowDays) when SWE > 10 mm of water equivalent (w.e.). It is

important to note that SnowDays are not necessarily continuous, with sporadic snow events occurring all year-round. van der Schot et al. (2024) ~~provides~~provide a thorough validation of CARRA SWE with in situ observations across Greenland. They
255 report that CARRA is capable of successfully representing snow-related indicators such as SWE_{MAX} and SWE_{MAX} DOY.

We calculated GrowDays by considering days that do not belong to SnowDays, with daily-averaged 2 m ~~air-temperature~~air temperature (T_{2m}) > 1 °C. The onset (i.e. the first) and termination (i.e. the last) day of the year of GrowDays are also derived. The indicator DegreeDays is obtained by summing up T_{2m} during the previously defined GrowDays. The daily rain ratio (RainRatio) is defined as the fraction of liquid precipitation of the total precipitation. SnowDays, in combination with
260 RainRatio higher than 50%, are used to derive days with rain-on-snow (RainOnSnow) between January and ~~September~~July to
investigate potential snowpack warming before the thermal growing season onset. SWE_{MAX} DOY and thermal growing season onset are used to determine the length of the snow melting period(~~$SWE_{meltDays}$~~). ~~Dividing SWE_{MAX} by $SWE_{meltDays}$, we estimate the averaged snow melting rate~~. During the snow melting period, we calculated daily changes of SWE from which we derived days with negative SWE changes ($SWE_{meltDays}$) and the mean of the negative SWE changes (MeltRate).

265 Certain bio-climatic indicators used in this study are based on seasonal statistics using the definition of meteorological seasons: winter includes December to February (DJF), spring from March to May (MAM), summer from June to August (JJA) and autumn from September to November (SON). Spectral greenness, T_{2m} , RainRatio, the volumetric soil water and ice (SoilWater and SoilIce) and vapour pressure deficit (VPd) are seasonally averaged, whereas precipitation, snowfall (Snow) and rainfall (Rain) are seasonally accumulated.

270 The vapour pressure deficit in summer (VPdJJA), which is the difference between the water vapour pressure of saturated air and the actual water vapour pressure in the air, was calculated to represent continentality. Continentality in summer is expressed by high temperatures and lower humidity due to large distances to moisture sources. This lack of moisture availability contributes to lower water vapour pressure, which, when combined with high temperatures, leads to higher VPd. A high VPdJJA indicates a strong drying potential in the atmosphere, which can significantly influence evaporation rates and plant water stress
275 (e.g., Grossiord et al. 2020; Yuan et al. 2019).

DroughtDays, the number of days with precipitation lower than 1 mm w.e. lasting for more than 10 consecutive days, is seasonally aggregated in spring and summer. HeatDays are also seasonally aggregated in spring and summer, and they consist of the number of days exceeding the seasonal T_{2m} climatology for the period 1991-2023 by two standard deviations (2SD). As the 32-year period is fairly ~~normal~~normally distributed, +2SD are approximately equivalent to 97.5th percentile. FrostDays in
280 spring are derived in the absence of snow cover, jointly with negative T_{2m} days.

Spectral greenness was ~~narrowed-to~~compiled for summer, in order to capture the period with maximum solar radiation in Greenland and avoid snow-covered patches. Given the fact that shadow areas heavily impact reflectance, latitudes higher than 75°N are not considered due to low sun elevation. We ~~restriet~~restricted our study area to West and Northeast Greenland, as steep mountains, deep fjords, expansive glaciers, and extensive ice caps inhibit the method's applicability in Southeast
285 Greenland.

3.3 Ecoregions

Greenland extends for approximately 23 degrees of latitude, with temperature and precipitation rates varying considerably across latitudes and coasts (Westergaard-Nielsen et al., 2020). Due to the semi-permanent Icelandic Low and the steep topography, the Southeast coast receives more precipitation than the Southwest coast (e.g., Ettema et al. 2010; Fettweis et al. 2017).
290 In general, the West and East coasts exhibit different topographic features, from a topographically complex East contrasting with predominantly glacially eroded regions in the West (e.g., Karami et al. 2017; Anderson 2020). Nevertheless, both coasts comprise diverse fjord systems, that often channel the wind and shield inland areas against storms. Consequently, the north-facing slopes and the leeward side of these inland mountain systems receive reduced precipitation. Such coast-inland gradients are therefore complex, also influencing the distribution of permafrost and freshwater systems (e.g., Westergaard-Nielsen et al.
295 2018; Abermann et al. 2019). Not only precipitation, but also temperature, tends to decrease with latitude. Other factors known to shape the coastal climate are prominent ocean currents (e.g., East Greenland and North Atlantic current) as well as sea ice and fjord ice conditions (e.g., Westergaard-Nielsen et al. 2020; Shahi et al. 2023).

The Arctic tundra ecosystem, including Greenland, is typically separated at around 70°N into Low Arctic and High Arctic based on climatic and vegetation differences (Bliss et al., 1973). Greenland has also been mapped according to hydrology,
300 soil pH, percentage of water cover, floristic provinces and bioclimatic subzones (e.g., Walker et al. 2005). The former mapping partly relies on mean July temperature thresholds and positive degree ~~month~~monthly temperatures to classify subzones. However, the T_{2m} JJA has warmed at a median rate of approx. 1°C per decade since 1991 (Fig. [S2S6](#)), likely shaping plant community structure and distribution. Eythorsson et al. (2019) also shows that Köppen-Geiger classification and snow cover frequency in the Arctic have changed and will continue to change in the Arctic this century. In order to avoid time varying
305 metrics, we split ice-free Greenland into five ecoregions (Fig. 1) based on physiogeographic features, such as adjacent seas, ocean currents and ice caps, with direct and indirect control on heat and moisture transport.

Ecoregion 1 is the narrow coast along the Baffin Bay in Northwest Greenland, including Sigguup Nunaa, Uummannaq fjord, Nuussuaq Peninsula and Disko Island. Disko Island is known as the transition region between High Arctic to Low Arctic, with a smooth transition of High Arctic to Low Arctic vegetation type in between ecoregions 1 and 2. Ecoregion 2 stretches from
310 Ilulissat to the Maniitsoq Ice Cap. This ice-free part is particularly widely stretched from West to East, with climates ranging from maritime at the coast to continental in the dry interior. Ecoregion 3 encloses mainly Southwest Greenland along the Labrador Sea until Nunarsuit, curving from the Labrador Sea to the North Atlantic. ~~The~~ Ecoregion 4 comprises the mountainous and southernmost end of Greenland, facing the North Atlantic. Southeast Greenland, a very narrow coast composed of steep slopes, is the meeting point between the relatively cold East Greenland current and the relatively warm Irminger Current,
315 leading to very foggy conditions during the warm season (e.g., Gilson et al. 2024; Laird et al. 2024). The combination of this region's complex topography with frequent cloud cover resulted in its exclusion from the analysis. Finally, ecoregion 5 spans from Kangertittivaq (Scoresby Sound) to the North coast of Young Sound, including Daneborg and Zackenberg. The coast of ecoregion 5 is also commonly affected by fog conditions. However, the coastal topography usually shelters inland regions. The

320 Stauning Alps, the large system of mountain ranges west of Kangertittivaq, is excluded due to its very rugged and complex topography, with numerous rocky peaks and active glaciers in most valleys and only minor vegetation growth.

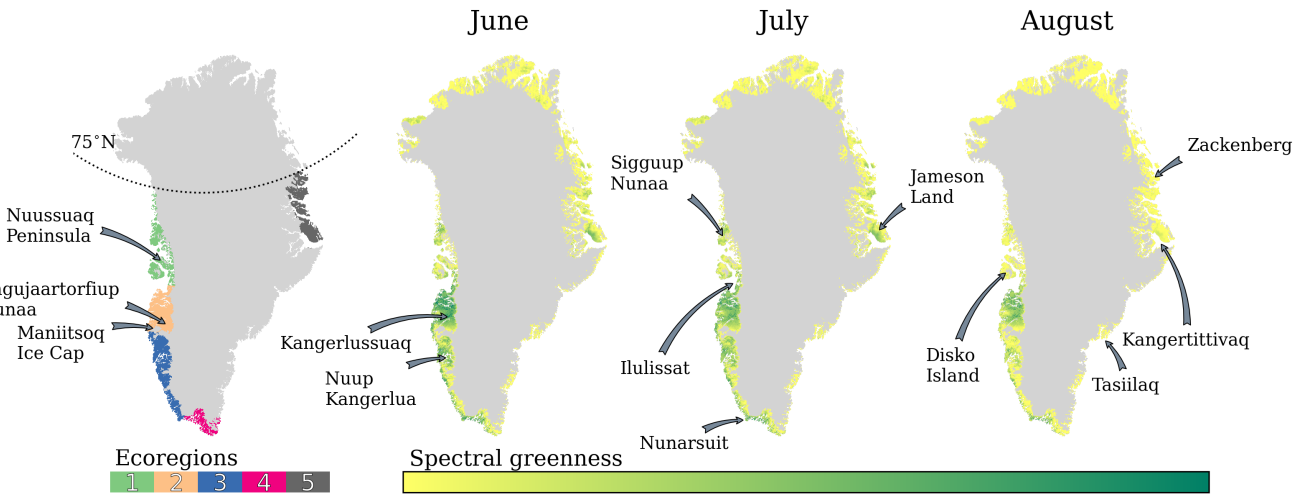


Figure 1. Averaged spectral greenness (based on the period 1991–2023) for Ecoregions in ice-free Greenland; June, July and August (upper panel) averaged spectral greenness for the period 1991–2023. No scale shown in the colour bar because the aim is to illustrate spectral greenness patterns, not absolute values; ecoregions in ice-free Greenland (lower-left panel); Pearson correlation coefficient between the summer averaged vegetation and the Greenland Blocking Index (GBI, lower-central panel), and the North Atlantic Oscillation (NAO, lower right panel). Place names Place names referenced in the study are displayed indicated.

The onset of the thermal growing season is inherently linked with distance to coast, elevation and latitude. While distance to coast and elevation control precipitation and snow depth, latitude controls sunlight duration and near-surface air temperature. Due to less elevated and less topographically complex terrain, the thermal growing season starts earlier at the West (on average [5th percentile, 95th percentile], DOY: 140 [103, 172]) than at the East Coast (DOY: 171 [145, 204]). Moreover, both latitude and elevation are crucial in cooling the atmosphere, allowing snowfall to occur, which in turn marks the end of the thermal growing season. The ecoregion with the most GrowDays is ecoregion 4 (140[76, 198] days), followed by ecoregion 2 and 3 (119 [75, 145] and 121 [77, 164] days), with less than 100 GrowDays in ecoregion 1 and 5 (97 [56, 132] and 78 [47, 108]). Due to the proximity to the Atlantic cyclone track, ecoregion 4 receives the most precipitation, accumulating to SWE_{MAX} of 432 [114, 984] mm w.e. In contrast, ecoregion 2 receives about 25% of the precipitation received by ecoregion 4, with SWE_{MAX} of 143 [64, 325] mm w.e. This is due to the fact that the interior of ecoregion 2 is surrounded by high peaks in the south (e.g., Maniitsoq Ice Cap), serving as a physical barrier for poleward moisture transport.

The correlations between Greenness and North Atlantic Oscillation (NAO) index and the Greenland Blocking Index (GBI) are shown in Figure 4S7. NAO and GBI are well-known climate oscillations, frequently utilized to characterize the main atmospheric circulation pattern in the vicinity of Greenland. The NAO is determined by the surface pressure difference between the semi-permanent Subtropical (Azores) High and the semi-permanent Subpolar (Icelandic) Low (Hurrell et al., 2003), and

its sign indicates the intensity of the North Atlantic jet stream. The phase of the NAO can explain most of the heat and moisture transported poleward, as well as temperature and precipitation anomalies in the periphery of Greenland (Björk et al., 2018). The GBI ~~represents the average geopotential height at 500 over Greenland (Hanna et al., 2016). This index~~ reflects the prevailing atmospheric circulation pattern, quantifying the strength of heat and moisture transport over the Greenland region.

340 Consequently, the GBI shows a strong correlation with near-surface variables in summer (e.g., Hanna et al. 2013; Hanna et al. 2015), such as spectral greenness.

3.4 Statistical methods

Principal Component Analysis (PCA) ~~was used~~, Pearson 1901; Lorenz 1956, often used on remotely sensed and environmental data (e.g., Mills et al. 2013; Yan and Tinker 2006), was employed to investigate the combined influence among bio-climatic in-

345 dicators ~~on summer greenness changes. PCA (Pedregosa et al., 2011) with summer greenness. The PCA (Pedregosa et al., 2011) solver was selected based on the input data shape. As the number of features in the input data is much less than the number of samples (geographic pixels), a classical eigenvalue decomposition on the covariance matrix was run. The classic PCA approach~~ operates upon several assumptions, including I. linearity, which assumes that the relationships between variables can be adequately described by linear transformations; II. that there are no significant outliers in the data; III. that there is

350 homoscedasticity, meaning that variables have equal variance. In order to overcome heteroscedasticity, we standardized all variables for each ecoregion, ~~centring~~ centering the distribution around 0 and scaling it to a standard deviation of 1. We used quartiles and the interquartile range (IQR) to filter out values beyond the upper ($Q_3 + 3 \times \text{IQR}$) and lower outer ($Q_1 - 3 \times \text{IQR}$) fence, with Q_1 and Q_3 as first and third quartile, respectively. Finally, we run a PCA for a set of bio-climatic indicators in every ecoregion between 1991 and 2023 until at least 90% of the cumulative explained variance is reached, omitting components

355 contributing to minimal explained variance in order to accelerate the computation process.

As the classic PCA requires the variables to be linearly related, we calculated Pearson correlation coefficients to investigate bio-climatic indicators by ecoregion. However, Pearson correlation assumes that the data are stationary; that is, their statistical properties do not change over time. In order to avoid serial autocorrelation, we transform the data into non-stationary time series by linearly detrending the data before performing correlation. The calculated correlations are displayed in a correlation

360 matrix, and bio-climatic indicators with similar correlations are sorted with hierarchical clustering. This helped to visually discern bio-climatic indicators with comparable statistical relationships and supported on the empirical reduction of indicators accounting for the relevant physical and the ecological processes on the tundra ecosystems, later used as part of the PCA. This will diminish "noise", redundancy and ultimately boost the clarity of interactions across atmosphere-biosphere-cryosphere.

Due to a change of satellite sensor from 2014 onwards, we also investigated how PCA performs interannually and whether

365 there was a statistically significant change of the explained variance for years before and after 2014. The result is shown in Figure S8 for a set of 16 bioclimatic indicators, displaying that the two independent samples of explained variance have identical averages in all ecoregions, with a 95 % confidence level, as determined by a two-sample t-test.

We attempt a careful causal interpretation of the loading vectors from the first two principal components (PCs) of the PCA through biplots (Gabriel, 1971). Although these PCs account for most of the explained variance, their interpretation in terms

370 of causality is limited by the nature of PCA as a descriptive statistical technique. For a cautious interpretation of the PCs, we examined not only the magnitude and direction of the loading vectors, but also trend maps of the involved bio-climatic indicators and literature on experimental studies.

We used the non-parametric Mann-Kendall (M-K) trend test (Hussain and Mahmud, 2019) to assess trend monotonicity and significance among bio-climatic indicators. However, to acknowledge autocorrelation in the greenness data, we computed the Hamed and Rao modified M-K test (Hamed and Rao, 1998), with a variance correction approach considering all significant lags to improve trend analysis. The trend magnitude retrieved over decadal timescales corresponds to the Theil-Sen (T-S) estimator, a robust regression method that does not require the data to be normally distributed, hence less vulnerable to outliers than conventional methods. Trends that exhibit Under the null hypothesis that the slope is equal to zero, trends exhibiting confidence levels higher than 90-95% are highlighted and treated as significant trends.

380 4 Results

The green vegetation extent has progressed at different rates across summer months and ecoregions (Fig. 2). Given the colder temperatures in ecoregions 1 (first column) and 5 (last column), vegetation growth was generally not evident until July, contrasting with the more southerly located ecoregions. However, as shown below in recent years, green vegetation extent was starting to increase already in June -in recent years, particularly noticeable for 2019. In the southern ecoregions, the thermal growing season onset (Onset) was much earlier, and some vegetation growth is seen began in the spring months. This is particularly especially pronounced in ecoregion 2, due to the typically shallow snow cover. By June, the vegetation was already quite developed, reaching its maximum extent in July. Ecoregion 2 comprises the largest vegetation extent, with vegetation covering approximately 80% of its area in 2015 and 2016.

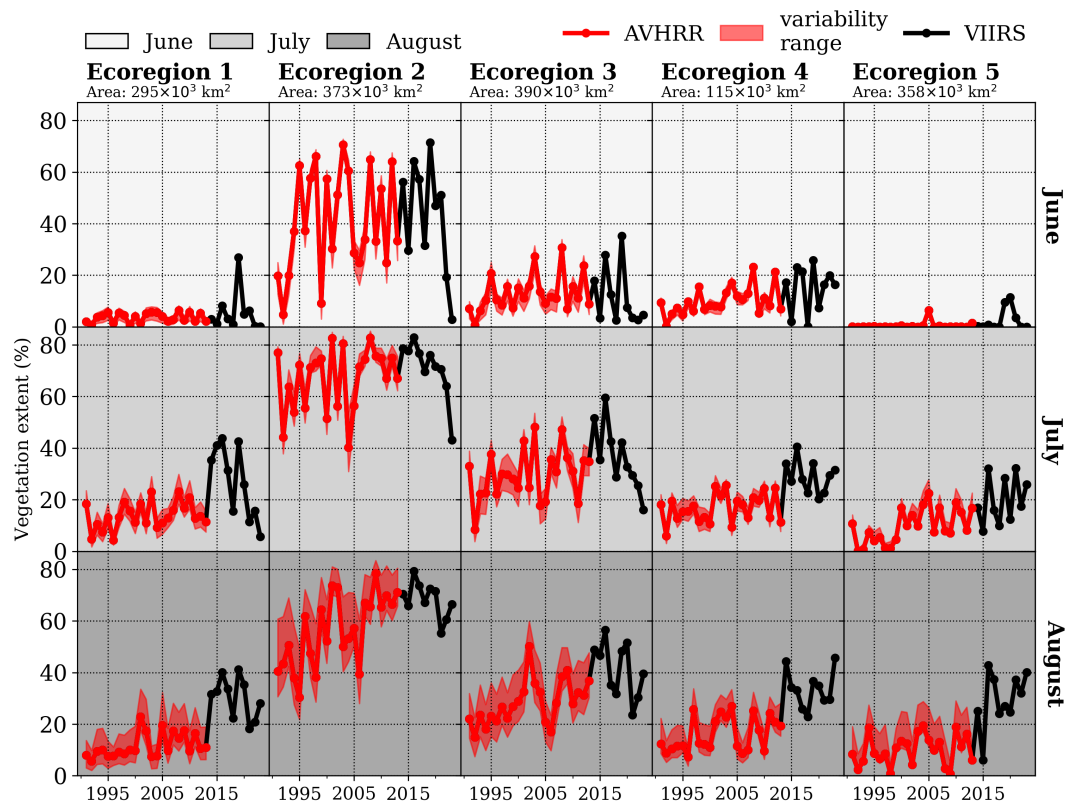


Figure 2. Development of green vegetation extent between 1991 and 2023 for June (upper row), July (middle row) and August (bottom row) across ecoregions based on AVHRR (red) and VIIRS (black). The AVHRR variability range is shaded in red, given the monthly minimum and maximum number of observations within VIIRS period (2014-2023).

It should be noted that prevailing weather patterns during summer months, like the North Atlantic Oscillation (NAO) and the Greenland Blocking Index (GBI), are highly correlated with spectral vegetation (Fig. S7). Therefore, summer weather patterns can accelerate or delay the maximum vegetation extent (Fig. 1). Significant green vegetation extent given their link with temperature and precipitation. Correlations between green vegetation extent and summer GBI are investigated for three periods: AVHRR (1991-2013), VIIRS (2014-2023) and the full period (1991-2023), and are shown in Table S1. Positive and significant correlation coefficients ranging between 0.5 and 0.8 are found between ecoregion 1 and 4, generally with higher correlations for VIIRS than for AVHRR period. Green vegetation extent in ecoregion 5 is poorly correlated with the prevailing weather patterns during summer.

While the AVHRR 22-year trend evidence general expansion of green vegetation, the VIIRS 9-year trend evidence decreases, particularly in West Greenland (Table S2). However, due to high variability and small sample size, most trends in both periods are not significant. Significant long-term trends in vegetation extent are not perceived, despite frequent, long-lasting and intense

400 ~~summer atmospheric blocking conditions in the past decades in the vicinity of Greenland.~~ trends range from 2 % per decade in
ecoregion 1 to approximately 6 % per decade in ecoregion 4.

4.1 Interconnectedness among bio-climatic indicators

~~As PCA requires the variables to be linearly related, we investigated the Pearson correlation coefficient among linearly~~
~~detrended bio-climatic indicators for each ecoregion separately. The result~~ The detrended Pearson correlation coefficients
405 for ecoregion 2 is shown in a correlation matrix in Fig. 3. The magnitude of the statistical links vary across ecoregions, but
the direction remains generally the same. ~~Here, bio-climatic indicators with similar correlations are sorted with hierarchical~~
~~clustering, which helps to visually discern bio-climatic indicators with comparable statistical relationships.~~

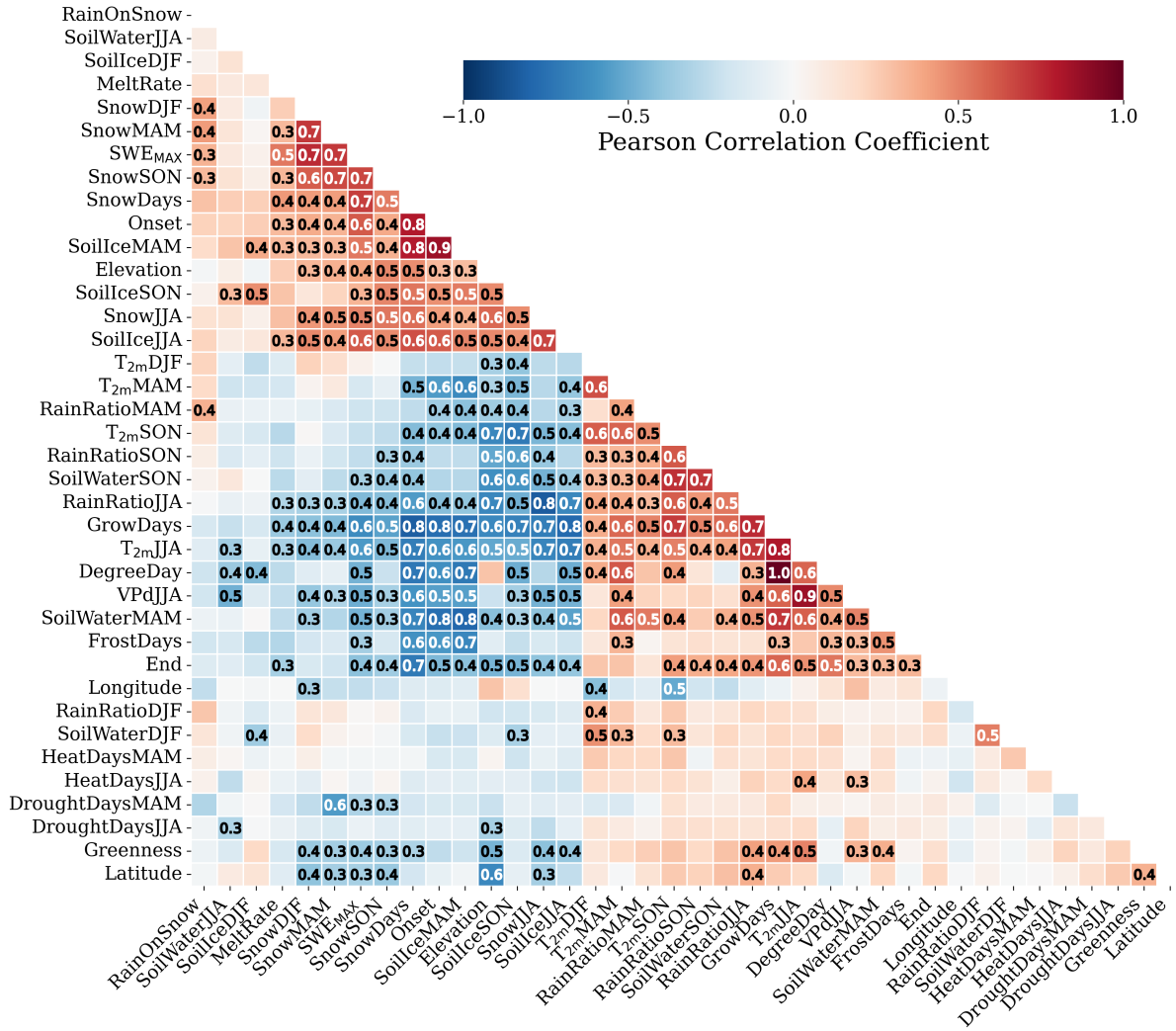


Figure 3. Correlation matrix for the bio-climatic indicators in [Ecoregion-ecoregion](#) 2, including Elevation, Longitude and Latitude. The correlation coefficient is colour-coded and the absolute value noted for absolute correlation coefficients higher than 0.3. The abbreviations of the bio-climatic indicators are described in Section 3.2 and in Table 1.

We investigated the correlations among all the bio-climatic indicators, including physical features like elevation, latitude and longitude. These physical features are connected to climate attributes across ecoregions. For instance, the higher the elevation and latitude, the lower the precipitation rates. It should be noted that these physical features are constant through time and were not considered when investigating the combined effect among bio-climatic indicators with greenness in the PCA.

A few bio-climatic indicators, such as DroughtDaysJJA, HeatDaysMAM, HeatDaysJJA, generally show correlations lower than 0.3, except DroughtDaysMAM that [significantly explains reductions in SnowMAM and partly in is negatively correlated with SnowMAM and with SWE_MAX](#). This indicates that the decrease in DroughtDaysMAM is accompanied by more frequent

415 ~~snowfall events, and not necessarily to more intense snowfall events. HeatDaysJJA are partly explained by HeatDaysJJA is~~
~~correlated with T_{2m} JJA, suggesting that the increased summer air-temperature in recent years near-surface air temperature~~
~~is associated with the increase of summer heat days. As greenness correlates stronger~~
~~We excluded drought and heat indicators~~
~~from the subsequent analysis, as greenness correlates more strongly~~
~~with seasonal temperatures and precipitation rates than with~~
~~the above-mentioned bio-climatic indicators, and since part of their variability is amounts. Also, drought and heat variability~~
420 ~~is respectively~~
~~explained by seasonal statistics, we excluded them from the subsequent analysis~~
~~temperature and precipitation.~~
~~However, it is important to highlight that the increase increases of Heat and DroughtDays in spring and summer are also~~
~~reflected by increased air-temperatures. This is because high-pressure systems, which are typically linked with clear skies,~~
~~occur more often and transport warm air from southern latitudes~~
~~near-surface air temperatures.~~
~~RainOnSnow seems to be~~
~~statistically~~
~~linked with the increase of the RainMAM and RainRatioMAM, but also with SnowMAM, as precipitation is likely~~
425 ~~RainRatioMAM represents~~
~~a mix of rain and snow. It In our trend analysis, it~~
~~is noticeable, that RainOnSnow is increasing along~~
~~East Greenland and FrostDays are locally increasing in West Greenland. However, summer spectral greenness , which is more~~
~~representative of resilient plant communities,~~
~~is not statistically responding to these two bio-climatic indicators. Therefore,~~
~~we removed them before from further analysis. Interestingly, FrostDays is positively correlated with spring near-surface air~~
~~temperature.~~
~~The increase in FrostDays is directly-linked also correlated~~
~~with early disappearance of the snow-cover and partly~~
430 ~~affected by shallower snowpacks . As surface and sub-surface melt is ongoing under snow-free days, FrostDays are , partly~~
~~related to shallower snowpacks and~~
~~highly correlated with the decreasing volume of ice in the soil in spring (SoilIceMAM).~~
~~SoilIce is to a large degree negatively correlated with the volume of water in the soil (SoilWater). Therefore, we decided to~~
~~arbitrarily~~
~~use SoilIce in winter (SoilIceDJF) and summer (SoilIceJJA) and SoilWater in spring (SoilWaterMAM) and autumn~~
~~(SoilWaterSON) in the further analysis. Additionally, SnowDays and DegreeDays are not used since both are highly explained~~
435 ~~by GrowDays. While DegreeDays sum up T_{2m} during GrowDays, SnowDays is complementary of GrowDays, FrostDays~~
~~and snow-free occasions with daily T_{2m} between 0 and 1 °C. In this way, we reduced the number of indicators that will be~~
~~used as part of the PCA, diminishing "noise" and boosting the explained variance across atmosphere-biosphere-cryosphere~~
~~interactions~~
~~Strong correlations between Rain and RainRatio are found in spring and autumn, but not in summer. Consequently,~~
~~we will retain both Rain and RainRatio variables exclusively for the summer. Finally, MeltRate is removed as it is physically~~
440 ~~explained by the snowpack depth.~~

4.2 Bio-climatic indicators ~~driving~~ interlinked with greenness

PCA was used to investigate the combined influence among bio-climatic indicators with summer spectral greenness. 16 bio-climatic indicators were chosen ~~that maximised the explained variance, whilst minimising redundant information to account for~~
~~the relevant physical and the ecological processes on the tundra ecosystem, as described in the Sections 3.4 and 4.1.~~ Figure 4
445 displays the combined influence of the 16 bio-climatic indicators based on the first two principal components across ecoregions.
These two principal components account for most of the variability, ranging from ~~51~~52% in ecoregion 2 to 65% in ecoregion 4
(Fig. S3). ~~Due to a change of satellite sensor from 2014 onwards, we investigated how PCA performs interannually and whether~~
~~there was a statistically significant change of the explained variance for years before and after 2014. The result is shown in~~

Figure S4, displaying that the two independent samples of explained variance have identical averages in all ecoregions, with a
450 90% confidence level, as determined by a two-sample t-test (S9). It takes more six to seven principal components to account for
additional 30 to 40% of the explained variance.

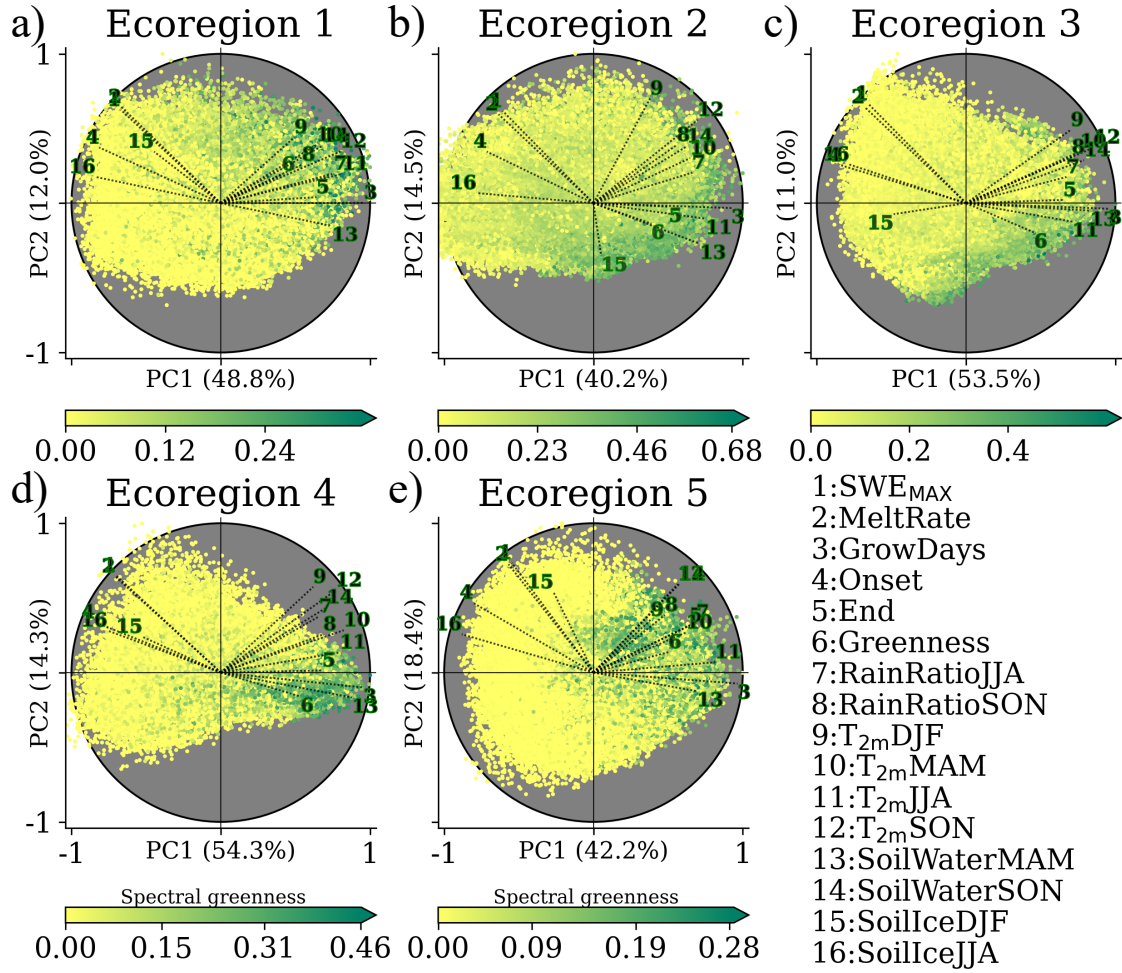


Figure 4. Biplot for scores between 1990–1991 and 2023 for each ecoregion. The loading vectors are labelled and scaled by the maximum of each principal component. The scores are colour-coded based on the summer spectral greenness as in Figure 1, with different scales to enhance greenness. The explained variance of the first (PC1) and second (PC2) component is labelled in the corresponding axis of the subplot. The 16 bio-climatic indicators are 1: maximum snow water equivalent (SWE_{MAX}); 2: averaged snow water equivalent melt rate (MeltRate); 3: total number of thermal growing days (GrowDays); 4–5: start (Onset) and termination (End) of GrowDays; 6: summer spectral greenness (Greenness); 7 and 8: averaged rain ratio in summer (RainRatioJJA) and autumn (RainRatioSON); 9, 10, 11, 12: averaged 2-m air temperature in winter ($T_{2m}DJF$), spring ($T_{2m}MAM$), summer ($T_{2m}JJA$) and autumn ($T_{2m}SON$); 13 and 14: volumetric soil water in spring and (SoilWaterMAM) autumn (SoilWaterSON); 15 and 16: volumetric soil ice in winter and (SoilIceDJF) summer (SoilIceJJA). The abbreviations of the bio-climatic indicators are described in Section 3.2 and in Table 1. The spatial pattern of the averaged 1991–2023 scores for both components in every ecoregion, including their corresponding loadings, are shown in Fig. S5–S9, S10–S14.

According to the spatial maps of the first (PC1) and second component (PC2) ~~spatial maps (Fig. S5-S9, Fig. S10-S14)~~, PC1 is found to be highly controlled by the topography of the ecoregion, and is consequently ~~dependent on~~ related to temperature (and through that on elevation), making GrowDays the bio-climatic indicator with the highest loading in all ecoregions, and therefore, the most significant contributor to the pattern represented by PC1. ~~The~~ Through the analysis of the trend map for RainJJA (Fig. S15) and the spatial maps of PC2 ~~is heavily shaped by continentality, permafrost extent and precipitation patterns, meaning that snow-related indicators, like we found that PC2 relates to precipitation and snow patterns, with SWE_{MAX} and MeltRate have RainJJA having~~ the highest explanatory power.

These two principal components together largely capture ~~and explain~~ Greenness distribution, as seen by scores with high summer spectral greenness often clustered in one specific quadrant of the biplot. ~~The wide range of conditions and locations of greenness could be related to different plant communities.~~ As GrowDays is the most important loading (displayed by the longest loading vector) across ecoregions, and given its small load along PC2, GrowDays ~~depends little on precipitation patterns.~~ shows little dependence on precipitation and snow patterns.

In ecoregion 2, the ecoregion with the widest East-West coverage, ~~greenness appears to extend from coastal to inland regions and summer greenness seems~~ summer greenness suggests to depend considerably on the snowpack of the preceding cold season (SWE_{MAX} loading vector opposite to Greenness loading vector). The decreasing trend of ~~snow rates (SnowDJF and SnowMAM seasonal accumulated snow (SnowDJF, Fig. S16 and SnowMAM, Fig. S17)~~ has led to SWE_{MAX}DOY to occur earlier. ~~Despite the increasing trend in T_{2m}MAM, the still-low solar elevation and the still-low near-surface air temperatures result in low~~ (Fig. S18), which resulted in lower melting rates of the snowpack (MeltRate). ~~These slow melt rates favour slow meltwater percolation as shown (Fig. S19).~~ These shallow snowpacks are statistically linked to more water content in the soil in spring (SoilWaterMAM loading vector opposite to ~~MeltRate~~ SWE_{MAX} loading vector). Additionally, the earlier snow depletion and thus earlier onset of the thermal growing season ~~allows vegetation to produce energy via photosynthesis, particularly in the ecoregions in lower latitudes with adequate sun exposure relates to enhanced spectral greenness~~ (Onset loading vector opposite to Greenness loading vector). A wide atmospheric warming, ~~that is assumed by the general increase is shown by increases~~ in T_{2m}JJA in most ecoregions (Fig. S2), ~~has resulted in~~ S6, which is also reflected on increases of RainRatioJJA, ~~despite the decrease of summer precipitation (Fig. S20).~~ These increases in RainRatioJJA do not seem to be linked to RainJJA between 1991 and 2023 (Fig. S10). ~~Therefore, increases of RainRatioJJA promote~~ 4 and Fig. S15). Likewise, RainJJA do not seem to be related to higher greenness (aligned loading vectors), as vegetation in such environmentally harsh places likely developed ~~mechanisms to effectively retain/absorb liquid water whenever possible.~~ Additionally orthogonal loading vectors in Fig. 4) across ecoregions. Also worth noting that RainJJA in the northern ecoregions is not in alignment with SoilIceJJA. In turn, the increase in T_{2m}JJA ~~generally favours~~ is generally aligned with less SoilIceJJA (opposed loading vectors). This is particularly evident in the northern ecoregions, ~~where summer rainfall has also increased, enhancing surface warming.~~ The remaining ecoregions show localized increases in SoilWaterJJA, which is in contrast with the significant decreases in ecoregion 2. ~~We attribute the decrease in SoilWaterJJA to higher rates of evaporation in the more continental areas of ecoregion 2, supported by the significant increase in VPdJJA in the region. The energy necessary to convert liquid water into water vapour (latent heat) cools down the soil. Despite increase in T_{2m}JJA (Fig. S21). The same areas in ecoregion 2, the little change found in~~

SoilHeeJJA trends reinforces this hypothesis. The presence of vegetation canopy from dwarf shrubs, that helps to shade the ground in summer, could be an additional aspect to consider for the preservation of SoilHeeJJA across permafrost areas in ecoregion 2. Also show significant increases in VPdJJA (Fig. S22). Additionally, the increased $T_{2m}SON$ is in alignment with the increase in RainRatioSON and SoilWaterSON. This is of great relevance for vegetation growth, particularly in the southern ecoregions, where the end of the thermal growing season comes occurs later.

We attempted to use the preceding autumn bio-climatic indicators to understand whether the start of the snow period could have played a role in the following growing season. However, the explained variance in PCA changed little (decreases of approx. 2-3% per ecoregion) and the relative importance of all loadings remained similar. Additionally, we correlated the interannual explained variance of the first two principal components with averaged climate oscillations (NAO and GBI) during the warm season (from March to September), spring and summer. We noted that the interannual change in explained variance is not significantly correlated with seasonal climate oscillations. In other words, a particular NAO or GBI phase does not boost the explained variance of the first principal components, maintaining the similar values interannually.

4.3 Coastal, latitudinal and altitudinal dependence on trends

The significant increase in length of the thermal growing season (GrowDays) across ice-free Greenland is shown in Figure 5. An evident increase in the number of GrowDays occurs in Southwest Greenland at low-laying regions below 600 meters above sea level (asl). At a local scale, significant increase is also found at elevations above 1000 m asl, more specifically within Nuup Kangerlua (east of Nuuk) and Angujaartorfiup Nunaa (in between Maniitsoq Ice Cap and Kangerlussuaq). Such areas are in precipitation shadows, with reduced snow depths, but close to glaciers and ice caps. Along the narrow ice-free stripes in the Southeast, there is a modest increase of GrowDays (approx. 5 days per decade), at several elevations around Tasiilaq. The most pronounced increase in the number of GrowDays occurs along the coast facing the Denmark Strait.

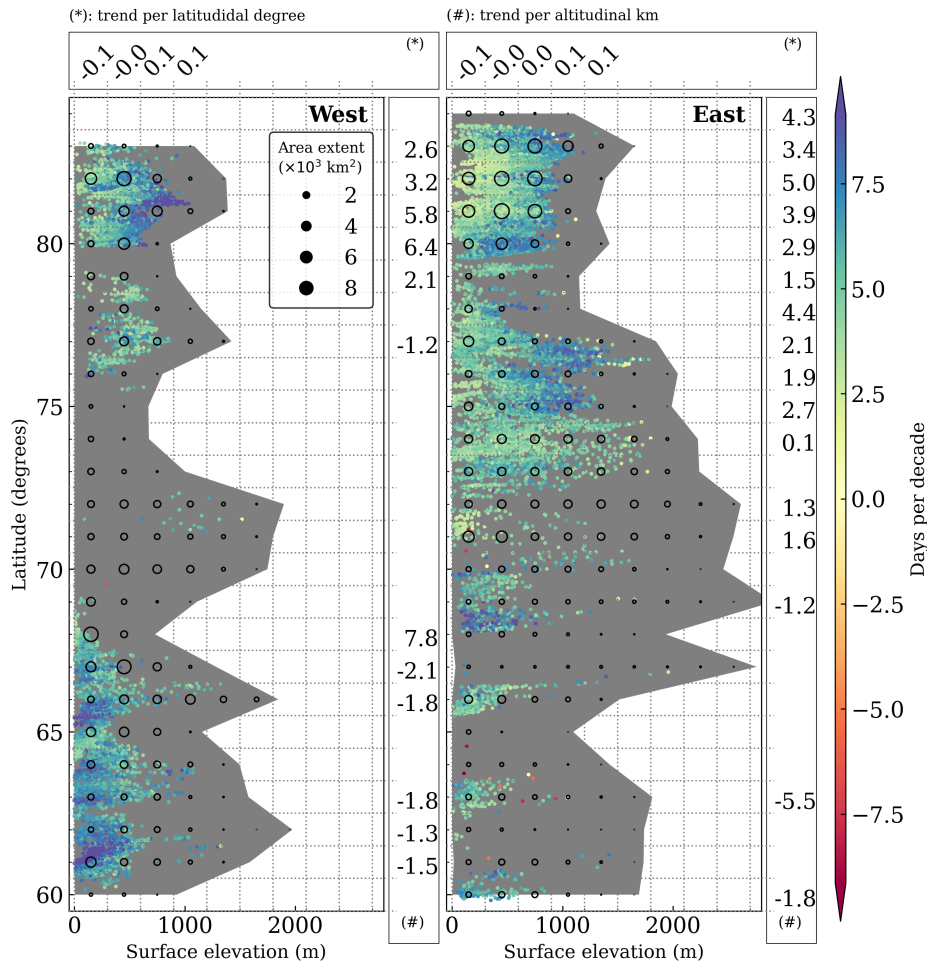


Figure 5. Significant trends for GrowDays (in days per decade) in the ice-free part of West (left panel) and East (right panel) Greenland. The trend's elevation dependency (in days per decade per altitudinal km) is binned in one degree of latitude and shown in vertical boxes marked with (#). The trend's latitudinal dependence (in days per decade per latitudinal degree) is binned every 300 m and shown in horizontal boxes marked with (*). The background grey shade displays the altitudinal extent of ice-free Greenland in the respective degree latitude, and the black circles represent the area extent by altitudinal and latitudinal bin. At least 50 pixels (approx. 312 km²) are required within each bin to compute its regression, otherwise not displayed. Trends are considered significant for confidence levels in the Mann-Kendall trend test higher than 9095%, with the null hypothesis that the slope is equal to zero.

The vast and relatively flat ice-free Jameson Land (east of Ittoqqortoormiit, between 70° and 72°N), shows little evidence of GrowDays change within the past three decades. At the northernmost part of ecoregion 5 (75°N), areas at low elevations reveal the smallest increase of GrowDays in the ecoregion. This feature becomes even more pronounced in Greenland's northernmost regions, exhibiting the highest GrowDays elevation sensitivity (approx. 5 days per decade per km elevation), which is a contrasting elevation dependence in comparison with Southern Greenland. This tendency is modestly evident for the latitudinal

sensitivity, mainly driven by high latitude and elevation trends: whereas GrowDays trends decrease with latitude in low-laying areas (< 300 m asl), GrowDays trends increase with latitude at higher elevations across North Greenland.

Trends for the onset of the thermal growing season resemble the trends in GrowDays, with earlier starts (approx. 8 days per decade) in southwest coastal Greenland and in the interior of Northeast Greenland. This comes as a consequence of shallower snow depths, that in combination with warming, has promoted longer snow-free periods. Thus, some areas of these ecoregions show increased trends in the number of frost days in spring. ~~The thermal growing season trends along ice-free Greenland (Fig. 5) reveal prolonged periods of snow-free conditions, allowing certain vegetation communities to grow and expand~~

~~The relationship between GrowDays and topographical features such as slope and aspect were further explored. As the surface slope is highly correlated with surface elevation, trends in GrowDays tend to significantly decrease with steepness. The dependence between GrowDays and surface aspect is rather complex, without a predominant slope orientation promoting GrowDays, in general.~~ However, ~~the increase in length of the thermal growing season is only one of several contributors to spectral greenness.~~ latitudes immediately south of Maniitsoq Ice Cap show increases of GrowDays in slopes with southwest orientation. On the East coast, a western slope orientation is particularly pronounced along Jameson Land, whereas northeast exposure appears favourable north of ecoregion 5. The dependence of the slope orientation for greenness changes is partly in alignment with the dependence of the slope orientation for GrowDays. Greenness trends increased in two latitudinal bands facing southeast in ecoregion 1 and 2. In Jameson Land a similar tendency for more greening is found towards southwest, while east facing slopes are preferred towards the northern part of ecoregion 5.

4.4 Greenness expansion and greening

Trends in summer spectral greenness are shown in Figure 6a. Significant greening occurs throughout Greenland, with pronounced greening across all ecoregions. Marked greening in ecoregion 1 is found in East Disko and northeast of Disko Bay. In ecoregion 2, the most pronounced greening is along the inland part of the Kangerlussuaq Fjord. The interior of Nuup Kangerlua ~~evidence shows~~ the highest greening in ecoregion 3. The coastal Kujalleq municipality, facing Labrador Sea, exhibits substantial greening. There are two greening clusters in ecoregion 5, being Jameson Land in the south, and the interior of King Christian X Land, in the north. In contrast, decreases in summer greenness are shown along the Southwest coast from ecoregion 1 to ecoregion 3, and in the interior of ecoregion 2.

In order to assess which regions became greener due to spectral vegetation expansion, we ~~annually~~ detected whether a pixel meets the spectral greenness criterion annually from 1991 to 2023. Then, we evenly split the study period into two and counted the total number of summers with spectral greenness within the two sub-periods. The result (Fig. 6c) shows the number of summers that are spectrally green in the second sub-period (2008-2023) with respect to the first sub-period (1991-2007), hereafter called changes in greenness distribution. The map of changes in greenness distribution shows that a considerable part of summer trends in spectral greening result from an expansion of vegetation. With the support of such a map, we discern that the relationship between changes in spectral greenness and its distribution are not linear. For instance, the central part of ecoregion 2 had as many summers of greenness in the second half as it had in the first half of the study period. Therefore, the changes in spectral greenness are either related to greening density of the existing vegetation or plant community change

in ecoregion 2. The increased trend in spectral greenness of the remaining areas seems to be the result of spectral greenness expansion, likely due to the colonization of previously bare ground. The decreased trend in spectral greenness along the coastal southwest suggests that spectral vegetation is not as dense in the second sub-period as it used to be. Also, vegetation seems to be emerging directly adjacent to the ice-sheet.

550 Figure 6b combines the information of both maps by displaying significant changes in greenness as a function of latitude and latitude, colour-coded by the changes in greenness distribution. Ecoregions 3 and 4 show shrinkage in greenness at elevations lower than 500 m, while ecoregion 2 shows shrinkage up to 1000 m at certain latitudinal bands. In contrast, expansion in greenness is not only shifting upward but also northward across all ecoregions, with notorious upward advancements south of Kangerlussuaq towards Angujaartorfiup Nunaa in the west and in Jameson Land in the east.

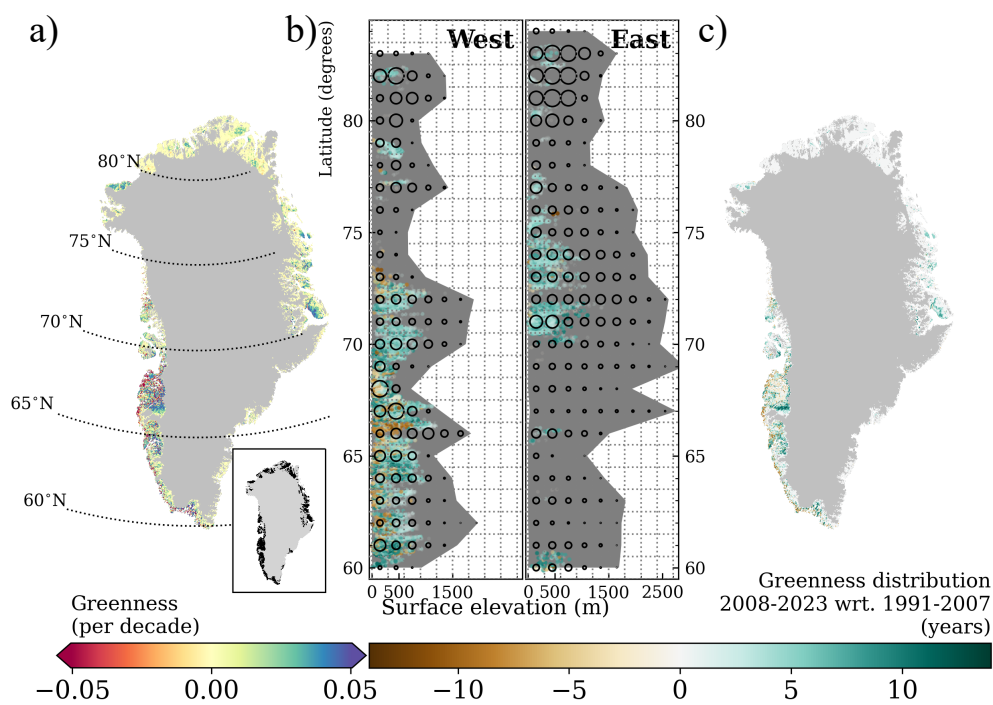


Figure 6. Trends in Greenness in Greenland (a). Significant trends are shown in the inset of (a) Trends are considered significant for confidence levels in the Mann-Kendall trend test higher than 99.95%, with the null hypothesis that the slope is equal to zero. Difference in summer greenness for the period 2008-2023 with respect to (wrt.) the period 1991-2007, called as changes in greenness distribution (c). Changes in greenness distribution as a function of latitude and elevation at locations with significant trends in spectral greenness in West and East ice-free Greenland (b). The background grey shade displays the altitudinal extent of ice-free Greenland in the respective degree latitude, and the black circles qualitatively represent the area extent by altitudinal and latitudinal bin.

555 According to Table 2, we show that ecoregion 2 experienced the highest greenness expansion at 44.2%, along with the highest greenness reduction at 33.4% between 2008-2023 compared to 1991-2007, resulting in an overall increase of 10.7% in vegetation greenness. Ecoregion 1 saw the largest increase in vegetation greenness at 22.2%, with a greenness expansion

of 30.6%. Ecoregion 5 had the lowest greenness reduction at 2.7% and an overall increase in vegetation greenness of 19.8%. Ecoregions 3 and 4 also experienced increases in vegetation greenness, at 18% and 20%, respectively.

Table 2. Percentage of vegetation expansion and shrinkage, and ratio (fraction of ~~expansion-expanded~~ by ~~shrinkageshrank area~~) between ~~2008-2023-2008 and 2023~~ with respect to ~~1991-2007-the period 1991–2007 in every-% of the total~~ ecoregion ~~area~~

	Ecoregion 1	Ecoregion 2	Ecoregion 3	Ecoregion 4	Ecoregion 5
Expansion	30.6	44.2	38.6	28.0	22.5
Shrinkage	8.4	33.4	20.5	7.9	2.7
Ratio	3.6	1.3	1.8	3.5	8.3

560 The southernmost and the northernmost ecoregions experience the highest expansion ratios, ranging from three times to eight times more expansion than shrinkage in ~~Ecoregion-ecoregion~~ 4 and 5, respectively. Overall, vegetation expansion in ice-free Greenland increases two times faster than vegetation reduction between 2008-2023 compared to 1991-2007.

5 Discussion

5.1 Key findings ~~and interpretation~~ in the context of the current literature

565 ~~For the first time~~, ~~Green vegetation has increased over time across Greenland, with an expansion rate of 2% per decade in ecoregion 1 to almost 5% per decade in ecoregion 4. When comparing the recent half of the time-series (2008–2023) to the distance half (1991–2007), the distribution of greenness has also changed. In ecoregion 3 and 5, greenness distributions expanded by almost two and eight times than the areas that shrank, respectively. Within the time-series, maximum green vegetation extent was observed in 2019, aligning with the end of a period of frequent, long-lasting and intense summer atmospheric blocking conditions in the vicinity of Greenland, conditions which promoted advection of relatively warm and humid air from the North Atlantic along West Greenland.~~

570 ~~atmospheric blocking conditions in the vicinity of Greenland, conditions which promoted advection of relatively warm and humid air from the North Atlantic along West Greenland.~~

~~To better understand how~~ bio-climatic indicators ~~co-varying co-varied~~ with spectral greenness ~~were statistically aggregated to better understand their combined relevance between 1991 and 2023 across ice-free Greenland. This is, a set of bio-climatic indicators including greenness were statistically aggregated. This was~~ achieved by using principal component analysis (PCA)

575 on remote-sensing data of spectral greenness and the output of a polar-adapted reanalysis. We demonstrated that the first two principal components account for most of the variability among the 16 combined bio-climatic indicators. These indicators were chosen to be of relevance to the ecological processes of tundra ecosystems. Given the fact that the chosen indicators are interlinked with supplementary indicators, we extended the interpretation to over 30 bio-climatic factors-

~~, with the support of climatology and trend maps.~~ PCA effectively clustered bio-climatic indicators that co-vary with sum-

580 mer spectral greenness ~~-Numerous indicators are closely correlated with air temperature based on data from 1991 to 2023. Numerous indicators closely co-vary with near-surface air temperature~~ and topography (PC1), and less on precipitation patterns (PC2), ~~except for ecoregion 2.~~ The rank of relative importance of individual bio-climatic indicators depends on ecoregion,

with the number of days of the thermal growing season (GrowDays) being the most relevant across all ecoregions. ~~Our results suggest that~~, followed by soil ice during summer (SoilIceJJA) in the northern and soil water in spring (SoilWaterMAM) in the southern ecoregions.

Our study found that areas related to green vegetation expansion in the northern ecoregions ~~, the reduction in soil ice during summer (SoilIceJJA) , due to warm and wet summers, is enabling vegetation growth, leading to northward expansion of vegetation. This reduction in SoilIceJJA is accompanied by substantial increases in air temperature (T_{2m} JJA) and the fraction of liquid precipitation (RainRatioJJA) during summer. However, due to the low precipitation rates at high latitudes, permafrost thawing is suggested as an important source of soil water availability. Regions have experienced a rise in SoilWaterMAM along with declines in both spring soil ice content trends (SoilIceMAM) and maximum snow depth (SWE_{MAX}). In Northwest Greenland, including ecoregion 1, regional exceptions of widespread increases in SWE_{MAX} with regional delays in the onset of the thermal growing season (Onset) are found along coastal areas and not related to spectral greening. Conversely, areas related to spectral greening are found linked with rising SoilWaterMAM, accompanied by higher spring temperatures (T_{2m} MAM) and earlier Onset. Despite regional trends on higher summer rainfall amounts (RainJJA, Niwano et al. 2021) in northern Greenland, we did not find a clear link between greening and changes in RainJJA. Interestingly, trends in summer soil water content (SoilWaterJJA) and soil ice content (SoilIceJJA) are both negatively related to near-surface air temperatures in summer (T_{2m} JJA). This results as a consequence of surface thawing and subsequently increased evaporation caused by higher vapour pressure deficits in these northern areas. The greening of the recently emerged vegetated areas in the northern ecoregions respond to different seasonal soil water contents. Greening in ecoregion 1 correlates best with SoilWaterMAM patterns, similar to the remaining southwestern ecoregions. Conversely, ecoregion 5 is more closely connected with SoilWaterJJA, likely due to a later onset of the GrowDays.~~

Southern ecoregions with significant decreases in ~~maximum snow water equivalent (SWE_{MAX}) evidence show~~ early SWE_{MAX} day of the year (DOY) that leads to early ~~onset of the GrowDays across ecoregions. Northwest Greenland, including ecoregion 1 is the only exception, where wide-spread increases in SWE_{MAX} along coastal areas has led to delays of the onset of the GrowDays~~Onset. Despite increased amounts of fresh snow and fewer drought days in spring ~~in Southwest Greenland (winter), the decreasing trend in SWE_{MAX} in ecoregions 3 and 4 is attributed to reduced winter snowfall. In most ecoregions (spring) snowfall in West (East) Greenland.~~

For most ecoregions in ice-free Greenland, we find that ~~shallower snowpacks melt at lower rates than deep snow. This has been mentioned in literature~~ snowpacks are becoming shallower, and consequently melt slowly, but earlier in the season. This feature was mentioned by Musselman et al. (2017) and is attributed to global warming. Musselman et al. (2017) explains that in Western North America ~~this is a consequence of the~~ regions with shallower snow are experiencing snow season contractions. Shallower snow is susceptible to snow season contraction ~~. Warmer near-surface temperatures in spring trigger and sustain slow snowmelt rates, as shallow snow depths require because shallow snow requires~~ less energy to initiate snowmelt melt than deeper snow. This earlier start of the ablation period occurs at a slower rate due to a combination of near-surface warming with relatively low solar altitude angles. In contrast, ~~for~~ deep snowpacks that require more energy to initiate melt, ~~are more likely to refreeze snowmelt water runoff, it is also more likely for the snowmelt water to refreeze~~ within

the snowpack (Dingman, 2015). Therefore, early season slow snowmelt rates in shallow snowpacks allow for efficient soil water absorption (Stephenson and Freeze, 1974), eventually used by microbial activity for percolation and subsequent water storage (Stephenson and Freeze, 1974). The successful percolation of liquid water into soil plays a key role in tundra regions during the snow ablation period and start of the growing season, as during this time soils are generally dry due to high drainage (Migala et al., 2014). Increased water availability in the soil could stimulate dormant microbial communities and thus increase the decomposition of soil organic matter ~~and then~~, releasing soil nutrients (Heijmans et al., 2022). ~~The combined effect of soil nutrients with increased soil water availability in spring~~ (e.g., Glanville et al. 2012; Salmon et al. 2016; Xu et al. 2021). This in turn could prime the soil for earlier and more efficient vegetation growth and colonization. The increased spring soil water content (SoilWaterMAM) ~~and T_{2m}MAM, promotes early plant growth~~, spring near-surface air temperature (T_{2m}MAM), and lengthening of the thermal growing season (GrowDays) indicated in our results could therefore improve conditions for plant growth and colonization, especially in the southern ecoregions. Therefore, ~~leaves~~ it is expected that plants are more developed in early summer, ~~which in association~~. Such conditions in conjunction with favourable weather patterns in summer associated with increased T_{2m}JJA and longer periods of solar radiation, ~~allow for greener vegetation~~ (Barrett et al., 2020), allowed for higher greenness levels and more green vegetation distribution. The same weather patterns also brought more drought and heat days, but apparently without an immediate negative impact on greenness.

The early onset of GrowDays has also contributed to local increases of freezing days (FrostDays) and rain on snow days (RainOnSnow). However, the effect of FrostDays is not reflected on greenness levels. This could be related to freezing episodes still during the dormant phase or rather short freezing episodes or a demonstration of certain plant community resilience (e.g., Gehrman et al. 2020; Körner and Alsos 2008). Nevertheless, the early onset of GrowDays allows vegetation to be potentially more active and responsive to solar radiation, particularly in the ecoregions in lower latitudes with longer sun exposure (Opała-Owczarek et al., 2018).

The drier conditions in the interior of ecoregion 2 have led to substantial losses in volumetric soil water during summer (SoilWaterJJA) with minimal changes in SoilIceJJA. We attribute the decrease in SoilWaterJJA to higher rates of evaporation in the more continental areas of the ecoregion, supported by the significant increase in vapour pressure deficit (VPdJJA, Fig. S22). The energy necessary to convert liquid water into water vapour (latent heat) cools down the soil. This is shown in our results where the increase in T_{2m}JJA and VPdJJA results in little changes in SoilIceJJA in ecoregion 2. This forces and limits vegetation distribution towards the proximity of water bodies. ~~Additionally, despite decreases in SoilWaterJJA~~ (Chen et al., 2023). Although there are no significant trends in SWE_{MAX} in ecoregion 2, ~~our results showed increased trends in spring and autumn as a result of slow snowmelt and increased rain ratio, respectively~~, subsurface runoff from ground thaw and meltwater from nearby snow/ice bodies likely contribute to the increase in SoilWaterMAM in the area. Episodic rainfall events in spring can also contribute to increased SoilWaterMAM. However, no significant changes in accumulated rain nor in rain ratio in spring (RainRatioMAM) were found in the region.

We report little to no change in the length and onset of the GrowDays along the coast in Northeast Greenland. In situ long-term measurements (e.g., Schmidt et al. 2023), state that some taxa may have reached their phenological limits despite ongoing warming. Assmann et al. (2019) suggests that temperature and snowmelt explain the effects on spring phenology in

Zackenberg, contrary to sea-ice break up in the Greenland Sea. However, the continuous southward transport of cold waters, frequently with sea ice, through the East Greenland current likely stabilizes the onset of the GrowDays at the coast. This seems to be corroborated given the dampened effect towards the interior and high elevations in Northeast Greenland, resulting in elevation sensitivity.

Grimes et al. (2024) investigated land cover changes across Greenland by using Landsat images since the late 1980s and found similar spatial patterns of vegetation change. For instance, they showed increases in coverage of vegetation southwest of Kangerlussuaq. They attributed this increase of vegetation to receding lakes happening, at least, since 1995 (Law et al., 2018). Similar to our findings, Grimes et al. (2024) detected increased vegetation cover in northeast of Kangerlussuaq. This has been shown and modelled in other parts of the Arctic tundra (e.g., Bosson et al. 2023; Jones and Henry 2003). Specifically, in ecoregion 2 and 5, green vegetation is not only expanding inland, but also upward. The interior of Greenland, less exposed to frontal systems developing over the Atlantic and with meltwater availability, seems to be favourable areas a more favourable area for vegetation growth. Although there are no significant trends in SWE_{MAX} in ecoregion 2, subsurface runoff from permafrost thaw and meltwater from nearby snow/ice bodies likely contribute to the increase in SoilWaterMAM in the area. Episodic rainfall events in spring can also contribute to increased SoilWaterMAM. However, no significant changes in accumulated rain nor in rain ratio in spring (RainRatioMAM) were found in the region as shown in ecoregion 1 and 2. Increasing greenness levels were also found with a tendency for slopes facing southeast in ecoregion 1 and 2. According to Grimes et al. (2024), the retreat of vegetation in front of the Maniitsoq Ice Cap is leading to the exposure of bedrock. Additionally, the less dense summer vegetation in coastal ecoregion 2 and along ecoregion 3 is suggested by Grimes et al. (2024) to be related to the increase increases in freshwater, likely due to increased river discharge. A small-scale study, north of Kangerlussuaq, reports declining growth of deciduous shrubs (Gamm et al., 2018) since the 1990s. A similar signal is seen regionally in our results. They reported that the decrease is likely due to water soil scarcity, being a markedly pronounced negative trend for SoilWaterJJA in the region. The derived spatio-temporal patterns of summer precipitation-rainfall (Fig. S10S15) and rain ratio (Fig. S20) are also in agreement with literature (e.g., Huai et al. 2022; van der Schot et al. 2023), especially on the significant increase of the rain ratio in North and West Greenland in summer and autumn. This consistency with other studies demonstrates the potential of the Copernicus Arctic regional reanalysis (CARRA) for biogeographic studies.

We report little to no change in the length and onset of the GrowDays along the coast in Northeast Greenland. In situ long-term measurements (e.g., Schmidt et al. 2023), state that some taxa may have reached their phenological limits despite ongoing warming. Assmann et al. (2019) suggests that temperature and snowmelt explain the effects on spring phenology in Zackenberg, contrary to sea-ice break up in the Greenland Sea. However, the continuous southward transport of cold waters, frequently with sea ice, through the East Greenland current likely stabilizes the onset of the GrowDays at the coast. This effect is dampened towards the interior and high elevations in Northeast Greenland, resulting in elevation sensitivity by extending insights from experimental studies into large-scale.

The wide-spread-widespread summer spectral greening occurs as a result of greener vegetation at certain sites. This likely occurred could be due to encroachment of vegetation on previously bare surfaces and changes in plant community composition at certain sites (Grimes et al., 2024). Spectral greenness correlates best with biophysical properties, such as leaf area index

(Myers-Smith et al., 2020). Therefore, we may argue that the spectral greening is generally related to tundra shrub expansion throughout the past three decades, as early proposed by Sturm et al. (2001).

690 5.2 ~~Implications~~Significance and implications

Longer thermal growing seasons are shown across Greenland between 1991 and 2023. Longer thermal growing seasons, associated with higher ~~air-temperatures, favour vegetation growth~~near-surface air temperatures have in the studied period favoured green vegetation growth and expansion. However, further investigation is required to comprehend the impacts on green vegetation and ecosystem functioning in regions that ~~may face severe freezing conditions in the future~~have been facing freezing
695 conditions due to reduced snow cover~~and changing precipitation patterns~~. Since our study determines a set of bio-climatic indicators relevant for spectral greenness, such insights can now be used to validate the same bio-climatic indicators retrieved from the historical period of global climate models to assess future vegetation changes across Greenland under a changing
700 climate, earlier onset of the thermal growing season as well as in regions exposed to heat stress conditions and changes in precipitation patterns throughout the thermal growing season. Given the reportedly significant decreases in snow cover, the surface albedo is lower for longer periods, facilitating more energy absorption and enhancing surface warming. The observed changes in greenness distribution enhance the surface albedo feedback, with varying effects that extend beyond the growing season and depended on the vegetation type (e.g., Blok et al. 2011; Loranty et al. 2011).

The surplus of the surface energy budget leads to surface warming and promotes surface thawing, particularly in the northern ecoregions. However, depending on the vapour pressure deficit and the vegetation canopy, the excess of surface energy can be
705 used for latent heat release, which in turn will cool the surface (Heijmans et al., 2022). The increase in green vegetation drives at first to greater carbon sequestration. However, if the increase in vegetation causes substantial surface thaw, the net effect could trigger the release of carbon, offsetting the compensation of carbon sequestration from vegetation (Glanville et al., 2012).

The terrestrial Arctic biosphere is an important regional source of primary biological aerosol particles (PBAPs), highly
710 correlated with ~~air-temperature~~near-surface air temperature and surface vegetation. These aerosol particles were found to play an important role in cloud formation, specifically in the Arctic with low aerosol concentrations (e.g., Pereira Freitas et al. 2023; Sze et al. 2022). Therefore, the increased ~~air-temperature~~near-surface air temperature and changes in vegetation can significantly impact cloud properties, such as cloud phase, radiative properties, cloud lifetime, and precipitation patterns, which in turn impact the surface conditions.~~Such PBAPs can be advected towards snow- and ice-covered regions, for instance~~
715 ~~the Greenland ice sheet, contributing to the surface darkening and enhancing algae growth~~ (Feng et al. 2024) which again leads to increased melt, particularly of the ice bodies in the vicinity of densely vegetated regions.

~~With decreasing sea ice, fog conditions are~~, including the surface energy budget. Additionally, low clouds and fog are
also very likely to become more frequent in certain coastal parts of Greenland (~~Song et al., 2023~~).due to decreasing sea ice (Song et al., 2023). The potential warming and shading conditions were shown through an experimental study in West
720 Greenland to reduce carbon sequestration from vegetation (Dahl et al., 2017). Water droplets from fog can effectively be retained by tundra vegetation and are not accounted as a water source. This interaction between fog, vegetation and soil conditions

should be better investigated ~~in~~ particularly for coastal tundra vegetation. Such PBAPs can also be advected towards snow- and ice-covered regions, for instance the Greenland ice sheet, contributing to the surface darkening and enhancing algae growth (Feng et al. 2024) which again leads to increased melt, particularly of the ice bodies in the vicinity of densely vegetated regions.

725

Longer thermal growing season in regions with shallow soils could have also significant large-scale implications for biodiversity. Prolonged warmth may foster the proliferation of shrubs, leading to increased "shrubification" and potentially resulting in the homogenization of species compositions across these landscapes (Myers-Smith et al., 2011). ~~This ecological shift~~ In other regions with deeper and frozen soils, the active layer deepening could favour graminoids due to longer roots (van der Kolk et al., 2016). In case of permafrost degradation with deep infiltration (Liljedahl et al., 2016), graminoids would also be favoured. This ecological shifts might will also affect animal communities such as birds (Boelman et al., 2015) and arthropods (Høye et al., 2018). Ultimately, the increased growing season could create favourable conditions for invasive species to establish and spread, further threatening the native biodiversity and altering the delicate balance of these unique environments (e.g., Elmendorf et al. 2012; Pearson et al. 2013).

730

Our study determines a set of bio-climatic indicators that have been shown relevant for spectral greenness. The statistical interlink among these indicators is confirmed in experimental studies across the Arctic (e.g., Chen et al. 2023; Gamm et al. 2018 ; Grimes et al. 2024; Huai et al. 2022; Migala et al. 2014; Musselman et al. 2017; Opala-Owczarek et al. 2018; Schmidt et al. 2023 ; Stephenson and Freeze 1974; van der Schot et al. 2024), allowing the interpretation of our outcome to be expanded to large-scale, with apparent features dependent on the ecoregion and latitude. Such insights can now be used to validate whether the same bio-climatic indicators interdependence is captured during the historical period of global climate models. This would guarantee more confidence in the use of these indicators for the study of future vegetation changes across Greenland under a changing climate.

735

740

5.3 Study limitations and future research directions

There are limitations in the use of NDVI for the characterization of changes in plant communities (e.g., Myers-Smith et al. 2020). This includes that NDVI is good at capturing plant communities with a high composition of shrubs (e.g., Blok et al. 2011), but it is not as good at detecting communities with low infrared reflectance or sparsely vegetated areas. Our methods in combination with proposed approaches as in Karami et al. (2018) and Rudd et al. (2021), who categorized tundra vegetation classes across ice-free Greenland, would allow an optimal assessment of spatio-temporal changes among plant communities. However, the high spatial resolution of optical satellite images from Landsat 8 and Sentinel 2 are only collected for approximately ~~a one~~ a decade. Another limitation regarding the NDVI analysis is that pixels associated with certain vegetation types (e.g., wet tundra) may be misinterpreted by adjacent water bodies, likely influencing spectral vegetation extent and trend magnitudes of certain areas, such as ~~shown in~~ discussed for ecoregion 2. Additionally, certain low-lying strips near fjords are very narrow, potentially causing errors in pixel reflectance calculations due to limited spatial resolution. Remote-sense NDVI products highly ~~depends~~ depend on the weather conditions in order to retrieve surface reflectance. Occasions with snow, shadows and clouds are thus assumed to be evenly distributed through time. The NDVI datasets employed in this study are sourced from

750

755

two satellite products processed by NOAA, each utilizing a different type of sensor. Due to the absence of a temporal dataset overlap, the assessment of uncertainties was limited and potential for mismatches between the datasets cannot be discarded. This lack of a common calibration period raises concerns about the reliability of long-term time integrated NDVI analysis. Also, spectral greenness highly responds to the prevailing atmospheric circulation patterns. An exceptional period in frequency and intensity of anti-cyclonic activity between 2010 and 2019, promoted advection of relatively warm and humid air from the North Atlantic towards Southwest Greenland (Silva et al., 2022). Such periods have favoured exceptional vegetation growth across western ecoregions as shown in our results. Despite the frequency of prevailing atmospheric circulation patterns, there is a superimposed warming signal, with less cold conditions likely promoting vegetation growth that is poorly captured due to cloudiness.

~~Even though CARRA is able to capture spatio-temporal changes on relevant bio-climatic indicators influencing spectral greenness, the effect of shrub canopies on the ground conditions are likely not captured. This implies that potential feedback loops (e.g., Hallinger et al. 2010; Barrere et al. 2018), where shrub growth and expansion result in more snow trapping during winter, thereby enhancing winter soil insulation, increased microbial activity, and more soil organic matter in spring, along with greater shading in the following summer (Blok et al., 2010) cannot be assessed yet. Additionally, the vegetation type was recently considered as a strong predictor of summer surface turbulent fluxes, latent and sensible heat fluxes (Oehri et al., 2022). Such mechanisms must be acknowledged for future projections of vegetation change in the Arctic. Also, the representativeness of the permafrost extent and active layer thickness will be key aspects to consider, as permafrost areas are rich in soil moisture and nutrients. Thus, areas under permafrost thawing are likely spots for future vegetation expansion, especially if the current trend in decreased summer precipitation remains. For the next decades, melting of glaciers and ice caps will also provide sediments and nutrients through increased runoff.~~

~~Soil~~The distribution of soil nutrients are also highly influenced by topography (not only elevation, but also relief and aspect), ~~reflected in vegetation but not entirely reflected on the vegetation changes in large-scale in our study~~. According to Anderson (2020), organic rich soils in Greenland generally accumulate on north facing slopes, with little to none on the south facing slopes as a result of precipitation patterns, whereas in valley bottoms and at slope breaks, thicker fen-like, organic rich deposits accumulate. Even though we have investigated how vegetation and bio-climatic indicators are changing as a function of latitude ~~and elevation~~, elevation, slope and aspect potential influences due to relief and aspect ~~should be considered, particularly apparent in our results, potentially more evident~~ at the local scale due to less spatial heterogeneity.

Our results show that summer spectral greenness appears statistically unresponsive to changes in rain on snow days (Rain-OnSnow) and below zero temperatures (FrostDays) during spring. Future work could rather focus on the analysis of extreme events and their impacts on greenness.

Even though CARRA is able to capture spatio-temporal changes on relevant bio-climatic indicators influencing spectral greenness, most implications, such as the effect of shrub canopies on the ground conditions are likely not captured. This implies that potential feedback loops (e.g., Hallinger et al. 2010; Barrere et al. 2018), where shrub growth and expansion result in more snow trapping during winter, thereby enhancing winter soil insulation (Lamichhane, 2021), increased microbial activity (Wang et al., 2024) along with greater shading in the following summer (Blok et al., 2010) cannot be properly assessed yet.

Additionally, the vegetation type was recently considered as a strong predictor of summer surface latent and sensible heat fluxes (Oehri et al., 2022). A better representation of the permafrost extent and active layer thickness together with the inclusion of dynamic tundra vegetation models within CARRA could be beneficial to deepen our knowledge on interactions among atmosphere, vegetation, carbon and nitrogen cycling, water and permafrost dynamics.

795 Permafrost areas will continue to likely be locations for future vegetation expansion (Chen et al., 2023), especially under the current trend of decreased summer precipitation. Moreover, permafrost thawed areas are also susceptible to fast drying (Liljedahl et al., 2016) and potentially sudden vegetation changes. Ultimately, plants can fixate along streams and small lakes as future land ice melt will continue to provide sediments and nutrients through runoff (Migala et al., 2014).

6 Conclusions

800 Our study aimed to better understand the long-term, large-scale interactions among various bio-climatic indicators and their collective effects ~~on-with~~ summer spectral greenness in ice-free Greenland. This study utilized remote sensing Normalized Difference Vegetation Index and bio-climatic indicators from the Copernicus Arctic regional reanalysis between 1991 and 2023. Bio-climatic changes are influenced by a complex set of factors, not only ~~centred-centered~~ in summer, but also dependent on winter and spring atmospheric temperatures, precipitation, solar radiation, soil properties, and soil water availability.

805 ~~Using an unsupervised method like principal component analysis, we successfully represented and described the relationship between bio-climatic indicators and summer greenness in accordance with both small- and large-scale observational studies. This analysis utilized remote sensing Normalized Difference Vegetation Index and bio-climatic indicators from the Copernicus Arctic regional reanalysis between 1991 and 2023. For this period, we identified a set of bio-climatic indicators that co-vary with summer spectral greenness across ecoregions. While the relative importance for most of these indicators is similar in~~

810 ~~different ecoregions, their-~~

We conclude that regions under green vegetation expansion in ice-free Greenland are associated with reductions in winter precipitation. The resulting shallower snowpacks melt earlier in the season but slower. This slow snowmelt rate allows the ground to retain more liquid water during the ablation period. Such conditions occur prior to the start of the thermal growing season are mentioned in experimental studies to facilitate vegetation growth. Longer thermal growing seasons accompanied

815 by prevailing summer weather patterns, with its peak in 2019, that promoted warmer and clear-sky conditions over the past decades also contributed to vegetation growth.

The spatio-temporal changes in summer greenness distribution depend on ecoregion, elevation and latitude. Overall, the bio-climatic changes during the study period led to more vegetation expansion, particularly towards the interior and northward; ~~rather than vegetation reduction.~~ Ultimately, this study encourages the incorporation of dynamic tundra vegetation schemes

820 to improve our knowledge on deeper interactions among atmosphere, vegetation, carbon and nitrogen cycling, water and permafrost dynamics, particularly for future projections.

Data availability. The Normalized Difference Vegetation Index CDR used in this study was acquired from NOAA's National Centers for Environmental Information (<http://www.ncei.noaa.gov><http://www.ncei.noaa.gov>). This CDR was originally developed by Eric Vermote and colleagues for NOAA's CDR Program.

825 Schyberg et al. (2020) was downloaded from the Copernicus Climate Change Service (2024). The results contain modified Copernicus Climate Change Service information 2024. Neither the European Commission nor ECMWF is responsible for any use that may be made of the Copernicus information or data it contains.

The North Atlantic Oscillation and Greenland Blocking Index data were obtained from the NCEP/CPC and the PSL/ESRL, respectively. Both climate oscillations were seasonally standardized relative to the period 1950-2000.

830 *Author contributions.* The inspiration for the paper was brought by BSW, EMB, IGA, JA and NdV, the concept and methodology was developed by TS, the original paper draft was written by TS, the data were processed and analyzed by TS, all authors contributed to the interpretation of results as well as reviewing and editing the final paper draft.

Competing interests. The authors declare that they have no conflict of interest.

Acknowledgements. The University of Graz is acknowledged for support of publication costs. Brandon S. Whitley, Elisabeth M. Biersma
835 and Natasha de Vere have received funding from the Carlsberg Foundation. The main author would like to acknowledge the use of OpenAI's ChatGPT for assisting in the writing and editing of this manuscript. The chatbot was utilized to enhance the clarity and readability of the text. A special thanks to Inger Greve Alsos and Therese Rieckh for their valuable suggestions.

References

- Aalto, J., Lehtonen, I., Pirinen, P., Aapala, K., and Heikkinen, R. K.: Bioclimate change across the protected area network of Finland, *Science of the Total Environment*, 893, 164 782, <https://doi.org/10.1016/j.scitotenv.2023.164782>, 2023.
- Abermann, J., Van As, D., Wacker, S., Langley, K., Machguth, H., and Fausto, R. S.: Strong contrast in mass and energy balance between a coastal mountain glacier and the Greenland ice sheet, *Journal of Glaciology*, 65, 263–269, <https://doi.org/10.1017/jog.2019.4>, 2019.
- Ackerman, D., Griffin, D., Hobbie, S. E., and Finlay, J. C.: Arctic shrub growth trajectories differ across soil moisture levels, *Global Change Biology*, 23, 4294–4302, <https://doi.org/10.1111/gcb.13677>, 2017.
- Anderson, N. J.: Terrestrial ecosystems of West Greenland, *Encyclopedia of the World's Biomes*, 1, 465–479, <https://doi.org/10.1016/B978-0-12-409548-9.12486-8>, 2020.
- Assmann, J. J., Myers-Smith, I. H., Phillimore, A. B., Bjorkman, A. D., Ennos, R. E., Prevéy, J. S., Henry, G. H., Schmidt, N. M., and Hollister, R. D.: Local snow melt and temperature—but not regional sea ice—explain variation in spring phenology in coastal Arctic tundra, *Global Change Biology*, 25, 2258–2274, <https://doi.org/https://doi.org/10.1111/gcb.14639>, 2019.
- Barrere, M., Domine, F., Belke-Brea, M., and Sarrazin, D.: Snowmelt events in autumn can reduce or cancel the soil warming effect of snow–vegetation interactions in the Arctic, *Journal of Climate*, 31, 9507–9518, <https://doi.org/10.1175/JCLI-D-18-0135.1>, 2018.
- Barrett, B. S., Henderson, G. R., McDonnell, E., Henry, M., and Mote, T.: Extreme Greenland blocking and high-latitude moisture transport, *Atmospheric Science Letters*, 21, e1002, <https://doi.org/10.1002/asl.1002>, 2020.
- Bengtsson, L., Andrae, U., Aspelien, T., Batrak, Y., Calvo, J., de Rooy, W., Gleeson, E., Hansen-Sass, B., Homleid, M., Hortal, M., Ivarsson, K.-I., Lenderink, G., Niemelä, S., Nielsen, K. P., Onvlee, J., Rontu, L., Samuelsson, P., Muñoz, D. S., Subias, A., Tijm, S., Toll, V., Yang, X., and Køltzow, M. Ø.: The HARMONIE–AROME model configuration in the ALADIN–HIRLAM NWP system, *Monthly Weather Review*, 145, 1919–1935, <https://doi.org/10.1175/MWR-D-16-0417.1>, 2017.
- Björk, A., Aagaard, S., Lütt, A., Khan, S., Box, J., Kjeldsen, K., Larsen, N., Korsgaard, N., Cappelen, J., Colgan, W., Machguth, H., Andresen, C. S., Y, P., and H, K. K.: Changes in Greenland's peripheral glaciers linked to the North Atlantic Oscillation, *Nature Climate Change*, 8, 48–52, <https://doi.org/10.1038/s41558-017-0029-1>, 2018.
- Bjorkman, A. D., Myers-Smith, I. H., Elmendorf, S. C., Normand, S., Rüger, N., Beck, P. S., Blach-Overgaard, A., Blok, D., Cornelissen, J. H. C., Forbes, B. C., et al.: Plant functional trait change across a warming tundra biome, *Nature*, 562, 57–62, <https://doi.org/10.1038/s41586-018-0563-7>, 2018.
- Bliss, L. C., Courtin, G., Pattie, D., Riewe, R., Whitfield, D., and Widden, P.: Arctic tundra ecosystems, *Annual Review of Ecology and Systematics*, pp. 359–399, 1973.
- Blok, D., Heijmans, M. M., Schaepman-Strub, G., Kononov, A., Maximov, T., and Berendse, F.: Shrub expansion may reduce summer permafrost thaw in Siberian tundra, *Global Change Biology*, 16, 1296–1305, <https://doi.org/10.1111/j.1365-2486.2009.02110.x>, 2010.
- Blok, D., Schaepman-Strub, G., Bartholomeus, H., Heijmans, M. M., Maximov, T. C., and Berendse, F.: The response of Arctic vegetation to the summer climate: relation between shrub cover, NDVI, surface albedo and temperature, *Environmental Research Letters*, 6, 035 502, <https://doi.org/10.1088/1748-9326/6/3/035502>, 2011.
- Boelman, N. T., Gough, L., Wingfield, J., Goetz, S., Asmus, A., Chmura, H. E., Krause, J. S., Perez, J. H., Sweet, S. K., and Guay, K. C.: Greater shrub dominance alters breeding habitat and food resources for migratory songbirds in Alaskan arctic tundra, *Global Change Biology*, 21, 1508–1520, <https://doi.org/10.1111/gcb.12761>, 2015.

- Boertmann, D., Olsen, K., and Nielsen, R. D.: Geese in Northeast and North Greenland as recorded on aerial surveys in 2008 and 2009, *Dansk Ornitologisk Forenings Tidsskrift*, 109, 206–17, 2015.
- Bosson, J.-B., Huss, M., Cauvy-Fraunié, S., Clément, J.-C., Costes, G., Fischer, M., Poulenard, J., and Arthaud, F.: Future emergence of new ecosystems caused by glacial retreat, *Nature*, 620, 562–569, <https://doi.org/10.1038/s41586-023-06302-2>, 2023.
- Chen, Y., Cheng, X., Liu, A., Chen, Q., and Wang, C.: Tracking lake drainage events and drained lake basin vegetation dynamics across the Arctic, *Nature Communications*, 14, 7359, <https://doi.org/10.1038/s41467-023-43207-0>, 2023.
- Colbeck, S. C.: An analysis of water flow in dry snow, *Water Resources Research*, 12, 523–527, 1976.
- Cooper, E. J.: Warmer shorter winters disrupt Arctic terrestrial ecosystems, *Annual Review of Ecology, Evolution, and Systematics*, 45, 271–295, <https://doi.org/10.1146/annurev-ecolsys-120213-091620>, 2014.
- Dahl, M. B., Priemé, A., Brejnrod, A., Brusvang, P., Lund, M., Nymand, J., Kramshøj, M., Ro-Poulsen, H., and Haugwitz, M. S.: Warming, shading and a moth outbreak reduce tundra carbon sink strength dramatically by changing plant cover and soil microbial activity, *Scientific Reports*, 7, 16035, <https://doi.org/10.1038/s41598-017-16007-y>, 2017.
- Dingman, S. L.: *Physical Hydrology*, Waveland press, 2015.
- Eikelenboom, M., Higgins, R. C., John, C., Kerby, J., Forchhammer, M. C., and Post, E.: Contrasting dynamical responses of sympatric caribou and muskoxen to winter weather and earlier spring green-up in the Arctic, *Food Webs*, 27, e00196, <https://doi.org/10.1016/j.fooweb.2021.e00196>, 2021.
- Elmendorf, S. C., Henry, G. H., Hollister, R. D., Björk, R. G., Boulanger-Lapointe, N., Cooper, E. J., Cornelissen, J. H., Day, T. A., Dorrepaal, E., Elumeeva, T. G., Gill, M., Gould, W. A., Harte, J., Hik, D. S., Hofgaard, A., Johnson, D. R., Johnstone, J. F., Jónsdóttir, I. S., Jorgenson, J. C., Klanderud, K., Klein, J. A., Koh, S., Kudo, G., Lara, M., Lévesque, E., Magnússon, B., May, J. L., Mercado-Díaz, J. A., Michelsen, A., Molau, U., Myers-Smith, I. H., Oberbauer, S. F., Onipchenko, V. G., Rixen, C., Schmidt, N. M., Shaver, G. R., Spasojevic, M. J., Þórhallsdóttir, t. E., Tolvanen, A., Troxler, T., Tweedie, C. E., Villareal, S., Wahren, C.-H., Walker, X., Webber, P. J., Welker, J. M., and Wipf, S.: Plot-scale evidence of tundra vegetation change and links to recent summer warming, *Nature Climate Change*, 2, 453–457, <https://doi.org/10.1038/nclimate1465>, 2012.
- Ettema, J., Van den Broeke, M., Van Meijgaard, E., and Van de Berg, W.: Climate of the Greenland ice sheet using a high-resolution climate model—Part 2: Near-surface climate and energy balance, *The Cryosphere*, 4, 529–544, <https://doi.org/10.5194/tc-4-529-2010>, 2010.
- Eythorsson, D., Gardarsson, S. M., Ahmad, S. K., Hossain, F., and Nijssen, B.: Arctic climate and snow cover trends—Comparing Global Circulation Models with remote sensing observations, *International Journal of Applied Earth Observation and Geoinformation*, 80, 71–81, <https://doi.org/10.1016/j.jag.2019.04.003>, 2019.
- Feng, S., Cook, J. M., Naegeli, K., Anesio, A. M., Benning, L. G., and Tranter, M.: The Impact of Bare Ice Duration and Geo-Topographical Factors on the Darkening of the Greenland Ice Sheet, *Geophysical Research Letters*, 51, e2023GL104894, <https://doi.org/10.1029/2023GL104894>, 2024.
- Fettweis, X., Box, J. E., Agosta, C., Amory, C., Kittel, C., Lang, C., van As, D., Machguth, H., and Gallée, H.: Reconstructions of the 1900–2015 Greenland ice sheet surface mass balance using the regional climate MAR model, *The Cryosphere*, 11, 1015–1033, <https://doi.org/10.5194/tc-11-1015-2017>, 2017.
- Franch, B., Vermote, E. F., Roger, J.-C., Murphy, E., Becker-Reshef, I., Justice, C., Claverie, M., Nagol, J., Csizar, I., Meyer, D., Baret, F., Masuoka, E., Wolfe, R., and Devadiga, S.: A 30+ year AVHRR land surface reflectance climate data record and its application to wheat yield monitoring, *Remote Sensing*, 9, 296, <https://doi.org/10.3390/rs9030296>, 2017.

- Gabriel, K. R.: The biplot graphic display of matrices with application to principal component analysis, *Biometrika*, 58, 453–467, <https://doi.org/10.1093/biomet/58.3.453>, 1971.
- Gamm, C. M., Sullivan, P. F., Buchwal, A., Dial, R. J., Young, A. B., Watts, D. A., Cahoon, S. M., Welker, J. M., and Post, E.: Declining growth of deciduous shrubs in the warming climate of continental western Greenland, *Journal of Ecology*, 106, 640–654, <https://doi.org/10.1111/1365-2745.12882>, 2018.
- Gandhi, G. M., Parthiban, S., Thummalu, N., and Christy, A.: Ndvi: Vegetation change detection using remote sensing and gis—A case study of Vellore District, *Procedia computer science*, 57, 1199–1210, <https://doi.org/10.1016/j.procs.2015.07.415>, 2015.
- Gehrmann, F., Lehtimäki, I.-M., Hänninen, H., and Saarinen, T.: Sub-Arctic alpine *Vaccinium vitis-idaea* exhibits resistance to strong variation in snowmelt timing and frost exposure, suggesting high resilience under climatic change, *Polar Biology*, 43, 1453–1467, <https://doi.org/10.1007/s00300-020-02721-3>, 2020.
- Gilson, G. F., Jiskoot, H., Gueye, S., and van Boxel, J. H.: A climatology of Arctic fog along the coast of East Greenland, *Quarterly Journal of the Royal Meteorological Society*, 150, 706–726, 2024.
- Glanville, H. C., Hill, P. W., Maccarone, L. D., N. Golyshin, P., Murphy, D. V., and Jones, D. L.: Temperature and water controls on vegetation emergence, microbial dynamics, and soil carbon and nitrogen fluxes in a high Arctic tundra ecosystem, *Functional Ecology*, 26, 1366–1380, <https://doi.org/10.1111/j.1365-2435.2012.02056.x>, 2012.
- Grimes, M., Carrivick, J. L., Smith, M. W., and Comber, A. J.: Land cover changes across Greenland dominated by a doubling of vegetation in three decades, *Scientific Reports*, 14, 3120, <https://doi.org/10.1038/s41598-024-52124-1>, 2024.
- Grossiord, C., Buckley, T. N., Cernusak, L. A., Novick, K. A., Poulter, B., Siegwolf, R. T., Sperry, J. S., and McDowell, N. G.: Plant responses to rising vapor pressure deficit, *New phytologist*, 226, 1550–1566, <https://doi.org/10.1111/nph.16485>, 2020.
- Hallinger, M., Manthey, M., and Wilmking, M.: Establishing a missing link: warm summers and winter snow cover promote shrub expansion into alpine tundra in Scandinavia, *New Phytologist*, 186, 890–899, <https://doi.org/10.1111/j.1469-8137.2010.03223.x>, 2010.
- Hamed, K. H. and Rao, A. R.: A modified Mann-Kendall trend test for autocorrelated data, *Journal of hydrology*, 204, 182–196, 1998.
- Hanna, E., Jones, J. M., Cappelen, J., Mernild, S. H., Wood, L., Steffen, K., and Huybrechts, P.: The influence of North Atlantic atmospheric and oceanic forcing effects on 1900–2010 Greenland summer climate and ice melt/runoff, *International Journal of Climatology*, 33, 862–880, <https://doi.org/10.1002/joc.3475>, 2013.
- Hanna, E., Cropper, T. E., Jones, P. D., Scaife, A. A., and Allan, R.: Recent seasonal asymmetric changes in the NAO (a marked summer decline and increased winter variability) and associated changes in the AO and Greenland Blocking Index, *International Journal of Climatology*, 35, 2540–2554, <https://doi.org/10.1002/joc.4157>, 2015.
- Hanna, E., Cropper, T. E., Hall, R. J., and Cappelen, J.: Greenland Blocking Index 1851–2015: a regional climate change signal, *International Journal of Climatology*, 36, 4847–4861, <https://doi.org/10.1002/joc.4673>, 2016.
- Heijmans, M. M., Magnússon, R. Í., Lara, M. J., Frost, G. V., Myers-Smith, I. H., van Huissteden, J., Jorgenson, M. T., Fedorov, A. N., Epstein, H. E., Lawrence, D. M., and Limpens, J.: Tundra vegetation change and impacts on permafrost, *Nature Reviews Earth & Environment*, 3, 68–84, <https://doi.org/10.1038/s43017-021-00233-0>, 2022.
- Hersbach, H., Bell, B., Berrisford, P., Hirahara, S., Horányi, A., Muñoz-Sabater, J., Nicolas, J., Peubey, C., Radu, R., Schepers, D., Simmons, A., Soci, C., Abdalla, S., Abellan, X., Balsamo, G., Bechtold, P., Biavati, G., Bidlot, J., Bonavita, M., De Chiara, G., Dahlgren, P., Dee, D., Diamantakis, M., Dragani, R., Flemming, J., Forbes, R., Fuentes, M., Geer, A., Haimberger, L., Healy, S., Hogan, R. J., Hólm, E., Janisková, M., Keeley, S., Laloyaux, P., Lopez, P., Lupu, C., Radnoti, G., de Rosnay, P., Rozum, I., Vamborg, F., Vil-

- laume, S., and Thépaut, J.-N.: The ERA5 global reanalysis, *Quarterly Journal of the Royal Meteorological Society*, 146, 1999–2049, <https://doi.org/10.1002/qj.3803>, 2020.
- 950 Høye, T. T., Bowden, J. J., Hansen, O. L., Hansen, R. R., Henriksen, T. N., Niebuhr, A., and Skytte, M. G.: Elevation modulates how Arctic arthropod communities are structured along local environmental gradients, *Polar Biology*, 41, 1555–1565, <https://doi.org/10.1007/s00300-017-2204-2>, 2018.
- Huai, B., van den Broeke, M. R., Reijmer, C. H., and Noël, B.: A daily 1-km resolution Greenland rainfall climatology (1958–2020) from statistical downscaling of a regional atmospheric climate model, *Journal of Geophysical Research: Atmospheres*, 127, e2022JD036688, <https://doi.org/10.1029/2022JD036688>, 2022.
- 955 Huang, M., Piao, S., Janssens, I. A., Zhu, Z., Wang, T., Wu, D., Ciais, P., Myneni, R. B., Peaucelle, M., Peng, S., Yang, H., and Peñuelas, J.: Velocity of change in vegetation productivity over northern high latitudes, *Nature Ecology & Evolution*, 1, 1649–1654, 2017.
- Hurrell, J. W., Kushnir, Y., Ottersen, G., and Visbeck, M.: An overview of the North Atlantic oscillation, *Geophysical Monograph-American Geophysical Union*, 134, 1–36, <https://doi.org/10.1029/134GM01>, 2003.
- 960 Hussain, M. and Mahmud, I.: pyMannKendall: a python package for non-parametric Mann Kendall family of trend tests., *Journal of Open Source Software*, 4, 1556, <https://doi.org/10.21105/joss.01556>, 2019.
- Jansen, E., Christensen, J. H., Dokken, T., Nisancioglu, K. H., Vinther, B. M., Capron, E., Guo, C., Jensen, M. F., Langen, P. L., Pedersen, R. A., Yang, S., Bentsen, M., Kjær, H. A., Sadatzki, H., Sessford, E., and Stendel, M.: Past perspectives on the present era of abrupt Arctic climate change, *Nature Climate Change*, 10, 714–721, 2020.
- 965 Jones, G. A. and Henry, G. H.: Primary plant succession on recently deglaciated terrain in the Canadian High Arctic, *Journal of Biogeography*, 30, 277–296, <https://doi.org/10.1046/j.1365-2699.2003.00818.x>, 2003.
- Kalnay, E., Kanamitsu, M., Kistler, R., Collins, W., Deaven, D., Gandin, L., Iredell, M., Saha, S., White, G., Woollen, J., Zhu, Y., Chelliah, M., Ebisuzaki, W., Higgins, W., Janowiak, J., Mo, K. C., Ropelewski, C., Wang, J., Leetmaa, A., Reynolds, R., Jenne, R., and Joseph, D.: The NCEP/NCAR 40-year reanalysis project, *Bulletin of the American meteorological Society*, 77, 437–472, [https://doi.org/10.1175/1520-0477\(1996\)077<0437:TNYP>2.0.CO;2](https://doi.org/10.1175/1520-0477(1996)077<0437:TNYP>2.0.CO;2), 1996.
- 970 Karami, M., Hansen, B. U., Westergaard-Nielsen, A., Abermann, J., Lund, M., Schmidt, N. M., and Elberling, B.: Vegetation phenology gradients along the west and east coasts of Greenland from 2001 to 2015, *Ambio*, 46, 94–105, <https://doi.org/10.1007/s13280-016-0866-6>, 2017.
- Karami, M., Westergaard-Nielsen, A., Normand, S., Treier, U. A., Elberling, B., and Hansen, B. U.: A phenology-based approach to the classification of Arctic tundra ecosystems in Greenland, *ISPRS Journal of Photogrammetry and Remote Sensing*, 146, 518–529, <https://doi.org/10.1016/j.isprsjprs.2018.11.005>, 2018.
- 975 Körner, C. and Alsos, I. G.: Freezing resistance in high arctic plant species of Svalbard in mid-summer, *Bauhinia*, 21, 1–8, 2008.
- Laird, N. F., Crossett, C. C., Keaton, G. A., and Hopson, L. N.: Weather conditions and seasonal variability of limited surface visibility at Greenland coastal locations, *International Journal of Climatology*, 44, 393–405, <https://doi.org/10.1002/joc.8332>, 2024.
- 980 Lamichhane, J. R.: Rising risks of late-spring frosts in a changing climate, *Nature Climate Change*, 11, 554–555, <https://doi.org/10.1038/s41558-021-01090-x>, 2021.
- Law, A., Nobajas, A., and Sangonzalo, R.: Heterogeneous changes in the surface area of lakes in the Kangerlussuaq area of southwestern Greenland between 1995 and 2017, *Arctic, Antarctic, and Alpine Research*, 50, S100027, <https://doi.org/10.1080/15230430.2018.1487744>, 2018.

- 985 Le Moullec, M., Sandal, L., Grøtan, V., Buchwal, A., and Hansen, B. B.: Climate synchronises shrub growth across a high-arctic archipelago: contrasting implications of summer and winter warming, *Oikos*, 129, 1012–1027, <https://doi.org/10.1111/oik.07059>, 2020.
- Liljedahl, A. K., Boike, J., Daanen, R. P., Fedorov, A. N., Frost, G. V., Grosse, G., Hinzman, L. D., Iijma, Y., Jorgenson, J. C., Matveyeva, N., et al.: Pan-Arctic ice-wedge degradation in warming permafrost and its influence on tundra hydrology, *Nature Geoscience*, 9, 312–318, <https://doi.org/10.1038/ngeo2674>, 2016.
- 990 Liu, Y., Wang, P., Elberling, B., and Westergaard-Nielsen, A.: Drivers of contemporary and future changes in Arctic seasonal transition dates for a tundra site in coastal Greenland, *Global Change Biology*, 30, e17 118, <https://doi.org/10.1111/gcb.17118>, 2024.
- Loranty, M. M., Goetz, S. J., and Beck, P. S.: Tundra vegetation effects on pan-Arctic albedo, *Environmental Research Letters*, 6, 024 014, <https://doi.org/10.1088/1748-9326/6/2/024014>, 2011.
- Lorenz, E. N.: Empirical orthogonal functions and statistical weather prediction, vol. 1, Massachusetts Institute of Technology, Department
995 of Meteorology Cambridge, 1956.
- Masson, V., Champeaux, J.-L., Chauvin, F., Meriguet, C., and Lacaze, R.: A global database of land surface parameters at 1-km resolution in meteorological and climate models, *Journal of Climate*, 16, 1261–1282, [https://doi.org/10.1175/1520-0442\(2003\)16<1261:AGDOLS>2.0.CO;2](https://doi.org/10.1175/1520-0442(2003)16<1261:AGDOLS>2.0.CO;2), 2003.
- Masson, V., Le Moigne, P., Martin, E., Faroux, S., Alias, A., Alkama, R., Belamari, S., Barbu, A., Boone, A., Bouysse, F., et al.: The
1000 SURFEXv7. 2 land and ocean surface platform for coupled or offline simulation of earth surface variables and fluxes, *Geoscientific Model Development*, 6, 929–960, <https://doi.org/10.5194/gmd-6-929-2013>, 2013.
- Mekonnen, Z. A., Riley, W. J., Berner, L. T., Bouskill, N. J., Torn, M. S., Iwahana, G., Breen, A. L., Myers-Smith, I. H., Criado, M. G., Liu, Y., et al.: Arctic tundra shrubification: a review of mechanisms and impacts on ecosystem carbon balance, *Environmental Research Letters*, 16, 053 001, <https://doi.org/10.1088/1748-9326/abf28b>, 2021.
- 1005 Metcalfe, D. B., Hermans, T. D., Ahlstrand, J., Becker, M., Berggren, M., Björk, R. G., Björkman, M. P., Blok, D., Chaudhary, N., Chisholm, C., Classen, A. T., Hasselquist, N. J., Jonsson, M., Kristensen, J. A., Kumordzi, B. B., Lee, H., Mayor, J. R., Prev  y, J., Pantazatou, K., Rousk, J., Sponseller, R. A., Sundqvist, M. K., Tang, J., Uddling, J., Wallin, G., Zhang, W., Ahlstr  m, A., Tenenbaum, D. E., and Abdi, A. M.: Patchy field sampling biases understanding of climate change impacts across the Arctic, *Nature Ecology & Evolution*, 2, 1443–1448, <https://doi.org/10.1038/s41559-018-0612-5>, 2018.
- 1010 Mig   a, K., Wojtu  n, B., Szyma  nski, W., and Muska  a, P.: Soil moisture and temperature variation under different types of tundra vegetation during the growing season: A case study from the Fuglebekken catchment, SW Spitsbergen, *Catena*, 116, 10–18, <https://doi.org/10.1016/j.catena.2013.12.007>, 2014.
- Mills, R. T., Kumar, J., Hoffman, F. M., Hargrove, W. W., Spruce, J. P., and Norman, S. P.: Identification and visualization of dominant patterns and anomalies in remotely sensed vegetation phenology using a parallel tool for principal components analysis, *Procedia Computer
1015 Science*, 18, 2396–2405, <https://doi.org/10.1016/j.procs.2013.05.411>, 2013.
- Musselman, K. N., Clark, M. P., Liu, C., Ikeda, K., and Rasmussen, R.: Slower snowmelt in a warmer world, *Nature Climate Change*, 7, 214–219, <https://doi.org/10.1038/nclimate3225>, 2017.
- Myers-Smith, I. H., Forbes, B. C., Wilmsking, M., Hallinger, M., Lantz, T., Blok, D., Tape, K. D., Macias-Fauria, M., Sass-Klaassen, U., L  vesque, E., Boudreau, S., Ropars, P., Hermanutz, L., Trant, A., Collier, L. S., Weijers, S., Rozema, J., Rayback, S. A., Schmidt, N. M.,
1020 Schaeppman-Strub, G., Wipf, S., Rixen, C., M  nard, C. B., Venn, S., Goetz, S., Andreu-Hayles, L., Elmendorf, S., Ravolainen, V., Welker, V., Grogan, P., Epstein, H. E., and Hik, D. S.: Shrub expansion in tundra ecosystems: dynamics, impacts and research priorities, *Environmental Research Letters*, 6, 045 509, <https://doi.org/10.1088/1748-9326/6/4/045509>, 2011.

- Myers-Smith, I. H., Kerby, J. T., Phoenix, G. K., Bjerke, J. W., Epstein, H. E., Assmann, J. J., John, C., Andreu-Hayles, L., Angers-Blondin, S., Beck, P. S., Berner, L. T., Bhatt, U. S., Bjorkman, A. D., Blok, D., Bryn, A., Christiansen, C. T., Cornelissen, J. H. C., Cunliffe, A. M.,
1025 Elmendorf, S. C., Forbes, B. C., Goetz, S. J., Hollister, R. D., de Jong, R., Loranty, M. M., Macias-Fauria, M., Maseyk, K., Normand, S., Olofsson, J., Parker, T. C., Parmentier, F.-J. W., Post, E., Schaepman-Strub, G., Stordal, F., Sullivan, P. F., Thomas, H. J. D., Tømmervik, H., Treharne, R., Tweedie, C. E., Walker, D. A., Wilmking, M., and Wipf, S.: Complexity revealed in the greening of the Arctic, *Nature Climate Change*, 10, 106–117, <https://doi.org/10.1038/s41558-019-0688-1>, 2020.
- Nachtergaele, F., van Velthuizen, H., Verelst, L., Batjes, N., Dijkshoorn, K., van Engelen, V., Fischer, G., Jones, A., and Montanarella, L.:
1030 The harmonized world soil database, in: *Proceedings of the 19th World Congress of Soil Science, Soil Solutions for a Changing World*, Brisbane, Australia, 1-6 August 2010, pp. 34–37, 2010.
- Niwano, M., Box, J., Wehrlé, A., Vandecrux, B., Colgan, W., and Cappelen, J.: Rainfall on the Greenland ice sheet: Present-day climatology from a high-resolution non-hydrostatic polar regional climate model, *Geophysical Research Letters*, 48, e2021GL092942, <https://doi.org/10.1029/2021GL092942>, 2021.
- 1035 Oehri, J., Schaepman-Strub, G., Kim, J.-S., Grysko, R., Kropp, H., Grünberg, I., Zemlianskii, V., Sonnentag, O., Euskirchen, E. S., Reji Chacko, M., Muscari, G., Blanken, P. D., Dean, J. F., di Sarra, A., Harding, R. J., Sobota, I., Kutzbach, L., Plekhanova, E., Riihimäki, A., Boike, J., Miller, N. B., Beringer, J., López-Blanco, E., Stoy, P. C., Sullivan, R. C., Kejna, M., Parmentier, F.-J. W., Gamon, J. A., Mastepanov, M., Wille, C., Jackowicz-Korczynski, M., Karger, D. N., Quinton, W. L., Putkonen, J., van As, D., Christensen, T. R., Hakuba, M. Z., Stone, R. S., Metzger, S., Vandecrux, B., Frost, G. V., Wild, M., Hansen, B., Meloni, D., Domine, F., te Beest, M., Sachs,
1040 T., Kalhori, A., Rocha, A. V., Williamson, S. N., Morris, S., Atchley, A. L., Essery, R., Runkle, B. R. K., Holl, D., Riihimäki, L. D., Iwata, H., Schuur, E. A. G., Cox, C. J., Grachev, A. A., McFadden, J. P., Fausto, R. S., Göckede, M., Ueyama, M., Pirk, N., de Boer, G., Bret-Harte, M. S., Leppäranta, M., Steffen, K., Friberg, T., Ohmura, A., Edgar, C. W., Olofsson, J., and Chambers, S. D.: Vegetation type is an important predictor of the arctic summer land surface energy budget, *Nature Communications*, 13, 6379, <https://doi.org/10.1038/s41467-022-34049-3>, 2022.
- 1045 Olafsson, H. and Rousta, I.: Influence of atmospheric patterns and North Atlantic Oscillation (NAO) on vegetation dynamics in Iceland using Remote Sensing, *European Journal of Remote Sensing*, 54, 351–363, <https://doi.org/10.1080/22797254.2021.1931462>, 2021.
- Opala-Owczarek, M., Pirożnikow, E., Owczarek, P., Szymański, W., Luks, B., Kępski, D., Szymanowski, M., Wojtuń, B., and Migala, K.: The influence of abiotic factors on the growth of two vascular plant species (*Saxifraga oppositifolia* and *Salix polaris*) in the High Arctic, *Catena*, 163, 219–232, <https://doi.org/10.1016/j.catena.2017.12.018>, 2018.
- 1050 Pearson, K.: LIII. On lines and planes of closest fit to systems of points in space, *The London, Edinburgh, and Dublin philosophical magazine and journal of science*, 2, 559–572, 1901.
- Pearson, R. G., Phillips, S. J., Loranty, M. M., Beck, P. S., Damoulas, T., Knight, S. J., and Goetz, S. J.: Shifts in Arctic vegetation and associated feedbacks under climate change, *Nature Climate Change*, 3, 673–677, <https://doi.org/10.1038/nclimate1858>, 2013.
- Pedregosa, F., Varoquaux, G., Gramfort, A., Michel, V., Thirion, B., Grisel, O., Blondel, M., Prettenhofer, P., Weiss, R., Dubourg, V.,
1055 Vanderplas, J., Passos, A., Cournapeau, D., Brucher, M., Perrot, M., and Duchesnay, E.: Scikit-learn: Machine Learning in Python, *Journal of Machine Learning Research*, 12, 2825–2830, <http://jmlr.org/papers/v12/pedregosa11a.html>, 2011.
- Pedron, S., Jespersen, R., Xu, X., Khazindar, Y., Welker, J., and Czimeczik, C.: More snow accelerates legacy carbon emissions from Arctic permafrost, *AGU Advances*, 4, e2023AV000942, <https://doi.org/10.1029/2023AV000942>, 2023.

- Pereira Freitas, G., Adachi, K., Conen, F., Heslin-Rees, D., Krejci, R., Tobo, Y., Yttri, K. E., and Zieger, P.: Regionally sourced bioaerosols drive high-temperature ice nucleating particles in the Arctic, *Nature Communications*, 14, 5997, <https://doi.org/10.1038/s41467-023-41696-7>, 2023.
- Post, E. and Pedersen, C.: Opposing plant community responses to warming with and without herbivores, *Proceedings of the National Academy of Sciences*, 105, 12 353–12 358, <https://doi.org/10.1073/pnas.0802421105>, 2008.
- Power, C. C., Normand, S., von Arx, G., Elberling, B., Corcoran, D., Krog, A. B., Bouvin, N. K., Treier, U. A., Westergaard-Nielsen, A., Liu, Y., and L. Prendin, A.: No effect of snow on shrub xylem traits: Insights from a snow-manipulation experiment on Disko Island, Greenland, *Science of The Total Environment*, 916, 169 896, <https://doi.org/10.1016/j.scitotenv.2024.169896>, 2024.
- Rantanen, M., Karpechko, A. Y., Lipponen, A., Nordling, K., Hyvärinen, O., Ruosteenoja, K., Vihma, T., and Laaksonen, A.: The Arctic has warmed nearly four times faster than the globe since 1979, *Communications Earth & Environment*, 3, 168, 2022.
- Rantanen, M., Kämäräinen, M., Niittynen, P., Phoenix, G. K., Lenoir, J., Maclean, I., Luoto, M., and Aalto, J.: Bioclimatic atlas of the terrestrial Arctic, *Scientific Data*, 10, 40, <https://doi.org/10.1038/s41597-023-01959-w>, 2023.
- Rawlins, M. A. and Karmalkar, A. V.: Regime shifts in Arctic terrestrial hydrology manifested from impacts of climate warming, *The Cryosphere*, 18, 1033–1052, <https://doi.org/10.5194/tc-18-1033-2024>, 2024.
- Rudd, D. A., Karami, M., and Fensholt, R.: Towards high-resolution land-cover classification of Greenland: A case study covering Kobbefjord, Disko and Zackenberg, *Remote Sensing*, 13, 3559, <https://doi.org/10.3390/rs13183559>, 2021.
- Salmon, V. G., Soucy, P., Mauritz, M., Celis, G., Natali, S. M., Mack, M. C., and Schuur, E. A.: Nitrogen availability increases in a tundra ecosystem during five years of experimental permafrost thaw, *Global Change Biology*, 22, 1927–1941, <https://doi.org/10.1111/gcb.13204>, 2016.
- Schmidt, N. M., Pedersen, S. H., Mosbacher, J. B., and Hansen, L. H.: Long-term patterns of muskox (*Ovibos moschatus*) demographics in high arctic Greenland, *Polar Biology*, 38, 1667–1675, <https://doi.org/10.1007/s00300-015-1733-9>, 2015.
- Schmidt, N. M., Reneerkens, J., Christensen, J. H., Olesen, M., and Roslin, T.: An ecosystem-wide reproductive failure with more snow in the Arctic, *PLoS Biology*, 17, e3000 392, <https://doi.org/10.1371/journal.pbio.3000392>, 2019.
- Schmidt, N. M., Kankaanpää, T., Tiisanen, M., Reneerkens, J., Versluijs, T. S., Hansen, L. H., Hansen, J., Gerlich, H. S., Høye, T. T., Cirtwill, A. R., Zhemchuzhnikov, M. K., Peña-Aguilera, P., and Roslin, T.: Little directional change in the timing of Arctic spring phenology over the past 25 years, *Current Biology*, 33, 3244–3249, <https://doi.org/10.1016/j.cub.2023.06.038>, 2023.
- Schyberg, H., Yang, X., Køltzow, M., Amstrup, B., Bakketun, m., Bazile, E., Bojarova, J., Box, J. E., Dahlgren, P., Hagelin, S., Homleid, M., Horányi, A., Høyer, J., Johansson, m., Killie, M., Körnich, H., Le Moigne, P., Lindskog, M., Manninen, T., Nielsen, E. P., Nielsen, K., Olsson, E., Palmason, B., Peralta, A. C., Randriamampianina, R., Samuelsson, P., Stappers, R., Støylen, E., Thorsteinsson, S., Valkonen, T., and Wang, Z.: Arctic regional reanalysis on single levels from 1991 to present. Copernicus Climate Change Service (C3S) Climate Data Store (CDS), <https://doi.org/10.24381/cds.713858f6>, accessed on 15-12-2022, 2020.
- Shahi, S., Abermann, J., Silva, T., Langley, K., Larsen, S. H., Mastepanov, M., and Schöner, W.: The importance of regional sea-ice variability for the coastal climate and near-surface temperature gradients in Northeast Greenland, *Weather and Climate Dynamics*, 4, 747–771, <https://doi.org/10.5194/wcd-4-747-2023>, 2023.
- Silva, T., Abermann, J., Noël, B., Shahi, S., van de Berg, W. J., and Schöner, W.: The impact of climate oscillations on the surface energy budget over the Greenland Ice Sheet in a changing climate, *The Cryosphere*, 16, 3375–3391, <https://doi.org/10.5194/tc-16-3375-2022>, 2022.

- Skakun, S., Justice, C. O., Vermote, E., and Roger, J.-C.: Transitioning from MODIS to VIIRS: an analysis of inter-consistency of NDVI data sets for agricultural monitoring, *International Journal of Remote Sensing*, 39, 971–992, <https://doi.org/10.1080/01431161.2017.1395970>, 2018.
- 1100 Søggaard, D. H., Lund-Hansen, L. C., López-Blanco, E., Schmidt, N. M., Winding, M. H. S., Sejr, M. K., Rysgaard, S., Sorrell, B. K., Christensen, T. R., Juul-Pedersen, T., Tank, J. L., and Riis, T.: Arctic coastal nutrient limitation linked to tundra greening, *Nature Communications*, 2023.
- Song, S., Chen, Y., Chen, X., Chen, C., Li, K.-F., Tung, K.-K., Shao, Q., Liu, Y., Wang, X., Yi, L., and Zhao, J.: Adapting to a Foggy Future Along Trans-Arctic Shipping Routes, *Geophysical Research Letters*, 50, e2022GL102395, <https://doi.org/10.1029/2022GL102395>, 2023.
- 1105 Stengel, M., Stapelberg, S., Sus, O., Finkensieper, S., Würzler, B., Philipp, D., Hollmann, R., Poulsen, C., Christensen, M., and McGarragh, G.: Cloud_cci Advanced Very High Resolution Radiometer post meridiem (AVHRR-PM) dataset version 3: 35-year climatology of global cloud and radiation properties, *Earth System Science Data*, 12, 41–60, <https://doi.org/10.5194/essd-12-41-2020>, 2020.
- Stephenson, G. R. and Freeze, R. A.: Mathematical simulation of subsurface flow contributions to snowmelt runoff, Reynolds Creek Watershed, Idaho, *Water Resources Research*, 10, 284–294, 1974.
- Sturm, M., Racine, C., and Tape, K.: Increasing shrub abundance in the Arctic, *Nature*, 411, 546–547, <https://doi.org/10.1038/35079180>, 1110 2001.
- Sze, K. C. H., Wex, H., Hartmann, M., Skov, H., Massling, A., Villanueva, D., and Stratmann, F.: Ice Nucleating Particles in Northern Greenland: annual cycles, biological contribution and parameterizations, *Atmospheric Chemistry and Physics Discussions*, 23, 1–45, <https://doi.org/10.5194/acp-23-4741-2023>, 2022.
- van der Kolk, H.-J., Heijmans, M. M., Van Huissteden, J., Pullens, J. W., and Berendse, F.: Potential Arctic tundra vegetation shifts in response to changing temperature, precipitation and permafrost thaw, *Biogeosciences*, 13, 6229–6245, <https://doi.org/10.5194/bg-13-6229-2016>, 1115 2016.
- van der Schot, J., Abermann, J., Silva, T., Jensen, C. D., Noël, B., and Schöner, W.: Precipitation trends (1958–2021) on Ammassalik island, south-east Greenland, *Frontiers in Earth Science*, 10, 1085499, <https://doi.org/10.3389/feart.2022.1085499>, 2023.
- van der Schot, J., Abermann, J., Silva, T., Rasmussen, K., Winkler, M., Langley, K., and Schöner, W.: Seasonal snow cover indicators in coastal Greenland from in situ observations, a climate model, and reanalysis, *The Cryosphere*, 18, 1033–1052, <https://doi.org/10.5194/tc-18-5803-2024>, 1120 2024.
- Vermote, E., Justice, C., Csaszar, I., Eidenshink, J., Myneni, R., Baret, F., Masuoka, E., Wolfe, R., Claverie, M., and Program, N. C.: NOAA Climate Data Record (CDR) of Normalized Difference Vegetation Index (NDVI), Version 5, <https://doi.org/10.7289/V5ZG6QH9>, access date: 2022-05-06, 2018.
- 1125 Vermote, E., Franch, B., Roger, J.-C., Murphy, E., Becker-Reshef, I., Justice, C., Claverie, M., Nagol, J., Csaszar, I., Meyer, D., Baret, F., Masuoka, E., Wolfe, R., Devadiga, S., Villaescusa, J., and Program, N. C.: NOAA Climate Data Record (CDR) of Surface Reflectance, Version 1, <https://doi.org/10.25921/gakh-st76>, access date: 2023-07-06, 2022.
- Walker, D. A., Raynolds, M. K., Daniëls, F. J., Einarsson, E., Elvebakk, A., Gould, W. A., Katenin, A. E., Kholod, S. S., Markon, C. J., Melnikov, E. S., Moskalenko, N. G., Talbot, S. S., Yurtsev, B. A., and other members of the CAVM Team, T.: The circumpolar Arctic vegetation map, *Journal of Vegetation Science*, 16, 267–282, <https://doi.org/10.1111/j.1654-1103.2005.tb02365.x>, 1130 2005.
- Wang, X., Li, Z., Xiao, J., Zhu, G., Tan, J., Zhang, Y., Ge, Y., and Che, T.: Snow cover duration delays spring green-up in the northern hemisphere the most for grasslands, *Agricultural and Forest Meteorology*, 355, 110130, <https://doi.org/10.1016/j.agrformet.2024.110130>, 2024.

- Weijers, S.: Declining temperature and increasing moisture sensitivity of shrub growth in the Low-Arctic erect dwarf-shrub tundra of western Greenland, *Ecology and Evolution*, 12, e9419, <https://doi.org/10.1002/ece3.9419>, 2022.
- Weijers, S., Buchwal, A., Blok, D., Löffler, J., and Elberling, B.: High Arctic summer warming tracked by increased *Cassiope tetragona* growth in the world's northernmost polar desert, *Global Change Biology*, 23, 5006–5020, <https://doi.org/10.1111/gcb.13747>, 2017.
- Westergaard-Nielsen, A., Karami, M., Hansen, B. U., Westermann, S., and Elberling, B.: Contrasting temperature trends across the ice-free part of Greenland, *Scientific Reports*, 8, 1586, <https://doi.org/10.1038/s41598-018-19992-w>, 2018.
- 1140 Westergaard-Nielsen, A., Hansen, B. U., Elberling, B., and Abermann, J.: Greenland Climates, *Encyclopedia of the World's Biomes*, 1, 465–479, <https://doi.org/10.1016/B978-0-12-409548-9.11750-6>, 2020.
- Xu, W., Prieme, A., Cooper, E. J., Mörsdorf, M. A., Semenchuk, P., Elberling, B., Grogan, P., and Ambus, P. L.: Deepened snow enhances gross nitrogen cycling among Pan-Arctic tundra soils during both winter and summer, *Soil Biology and Biochemistry*, 160, 108356, <https://doi.org/10.1016/j.soilbio.2021.108356>, 2021.
- 1145 Yan, W. and Tinker, N. A.: Biplot analysis of multi-environment trial data: Principles and applications, *Canadian journal of plant science*, 86, 623–645, <https://doi.org/10.4141/P05-169>, 2006.
- Yang, W., Tan, B., Huang, D., Rautiainen, M., Shabanov, N. V., Wang, Y., Privette, J. L., Huemmrich, K. F., Fensholt, R., Sandholt, I., Weiss, M., Ahl, D., Gower, S., Nemani, R., Knyazikhin, Y., and Myneni, R.: MODIS leaf area index products: From validation to algorithm improvement, *IEEE Transactions on Geoscience and Remote Sensing*, 44, 1885–1898, <https://doi.org/10.1109/TGRS.2006.871215>, 2006.
- 1150 Yuan, H., Dai, Y., Xiao, Z., Ji, D., and Shangguan, W.: Reprocessing the MODIS Leaf Area Index products for land surface and climate modelling, *Remote Sensing of Environment*, 115, 1171–1187, <https://doi.org/10.1016/j.rse.2011.01.001>, 2011.
- Yuan, W., Zheng, Y., Piao, S., Ciais, P., Lombardozzi, D., Wang, Y., Ryu, Y., Chen, G., Dong, W., Hu, Z., Jain, A. K., Jiang, C., Kato, E., Li, S., Lienert, S., Liu, S., Nabel, J. E., Qin, Z., Quine, T., Sitch, S., Smith, W. K., Wang, F., Wu, C., Xiao, Z., and Yang, S.: Increased atmospheric vapor pressure deficit reduces global vegetation growth, *Science advances*, 5, eaax1396, <https://doi.org/10.1126/sciadv.aax1396>, 2019.
- 1155 Zwolicki, A., Zmudczyńska-Skarbek, K., Wietrzyk-Pelka, P., and Convey, P.: High Arctic vegetation, *Encyclopedia of the World's Biomes*, 1, 465–479, <https://doi.org/10.1016/B978-0-12-409548-9.11771-3>, 2020.